

# Chapter 6

## Titanium Dioxide in Photocatalysis

S. Cassaignon, C. Colbeau-Justin and O. Durupthy

**Abstract** TiO<sub>2</sub>-based heterogeneous photocatalysis is a process that develops rapidly in environmental engineering and it is now employed in several industrial domains, including water treatment, air purification, and self-cleaning surfaces. Photocatalysis is a natural phenomenon in which the TiO<sub>2</sub> accelerates a chemical reaction through the action of light, without being altered. The illuminated TiO<sub>2</sub> induces the formation of reactive species, able to decompose by oxidation and/or reduction reactions organic or inorganic substances. The major part of the applications of photocatalysis corresponds to organic oxidation, and it is now considered as one of the Advanced Oxidation Technologies (AOTs), gathering the reactions mainly based on hydroxyl radical (HO<sup>•</sup>) chemistry. The development of a system based on photocatalysis requires gathering knowledge of numerous and various scientific domains: physical-chemistry, materials science, catalysis, environmental chemistry, biology, and engineering science. This chapter is therefore designed to give a detailed survey of the different scientific fields concerning TiO<sub>2</sub>-

---

S. Cassaignon (✉) · O. Durupthy  
Chimie de la Matière Condensée de Paris, UMR 7574, Collège de France, UPMC Univ Paris 06, 11 place Marcelin Berthelot, 75231 Paris Cedex 05, France  
e-mail: sophie.cassaignon@upmc.fr

S. Cassaignon · O. Durupthy  
CNRS, Chimie de la Matière Condensée de Paris, UMR 7574, Collège de France, 11 place Marcelin Berthelot, 75231 Paris Cedex 05, France

S. Cassaignon · O. Durupthy  
Chimie de la Matière Condensée de Paris, Collège de France, 11 place Marcelin Berthelot, 75231 Paris Cedex 05, France

C. Colbeau-Justin  
Laboratoire de Chimie Physique, UMR8000, Univ Paris-Sud, 91405 Orsay, France

C. Colbeau-Justin  
CNRS, Laboratoire de Chimie Physique, UMR8000, Univ Paris-Sud, 91405 Orsay, France

based photocatalysis. Various aspects are developed: materials (synthesis, crystal chemistry, electronic and optical properties of  $\text{TiO}_2$ ), physical-chemistry (photon absorption, charge-carrier dynamics, surface adsorption, and photooxidation mechanisms), environmental chemistry (dyes, pesticides, bacteria, and antibiotic photodegradation, real industrial wastewater treatment), and engineering (photocatalytic reactor design and simulation).

## 6.1 Introduction

Today more than ever, the human activity and modern life style are responsible for the worsening environmental pollution. Sources of pollution are becoming more numerous and diverse (industry, automobile, petroleum, waste plastics and computer, consumer products). The accumulation of gaseous or liquid exhausts provokes the pollution of the atmosphere as well as water resources. But air pollution is not limited to the outside, it includes also indoor where we spend about 90 % of our time.

Heterogeneous photocatalysis is a process that develops rapidly in environmental engineering and it is now employed in several industrial domains, including systems for (i) water depollution: water purification, treatment of industrial effluents in order to limit the release of toxic compounds, (ii) air depollution: destruction of bacteria that cause odor nuisance or that are present in hospital, reducing air pollution in an urban environment (conversion of  $\text{NO}_x$  to  $\text{NO}_3^-$ , then trapped in water), and also (iii) self-cleaning surfaces: increasing duration between cleaning of a surface. The main advantages of the photocatalysis are: low cost, ease of initiation and stopping the reaction, the low energy consumption, the variety of degradable pollutants, and a high efficiency in pollutants mineralization (conversion of organics to  $\text{H}_2\text{O}$ ,  $\text{CO}_2$  and  $\text{NO}_3^-$ ,  $\text{PO}_4^{3-}$ , halide ions, etc.)

Photocatalysis is a natural phenomenon (thermodynamically favored) in which a substance called photocatalyst accelerates a chemical reaction through the action of light (natural or artificial), without being altered. Using light energy, photocatalysts induce the formation of reactive species, able to decompose by oxidation and/or reduction reactions organic or inorganic substances. The mechanism of photocatalysis consists of four stages. (1) The photocatalysts are semiconductors, which can be excited by light with higher energy than the bandgap ( $h\nu > E_g$ ), and (2) energy-rich electron-hole pairs are formed which dissociate into free photoelectrons in the conduction band (CB) and photo-holes in the valence band (VB). Then (3), there is migration of the charge carriers toward the surface of material and simultaneously, in the presence of a fluid phase (gas or liquid), adsorption occurs spontaneously. (4) According to redox potential (or energy level) of each adsorbate, an electron transfer occurs to the molecules with acceptor character while the positive photo-holes are transferred to the molecules with donor

character. During the reaction of photodegradation, one or more reactive species of water or air may be implied ( $\text{HO}^\bullet$ ,  $\text{O}_2^{\bullet-}$ ,  $\text{H}_2\text{O}_2$ , etc.). The photocatalytic activity is controlled by several factors intrinsic to the material: (i) its coefficient and its range of optical absorption; (ii) the speed of reduction or oxidation on the surface by the electron and the hole; (iii) the rate of recombination of the electron-hole pair.

Several photocatalytic reactions have direct environmental applications. Such applications have played an important role in the development of photocatalysis, both as scientific discipline and industrial market.




The major part of those applications corresponds to organic oxidation, and photocatalysis is now considered as one of the Advanced Oxidation Technologies (AOTs). The AOTs are gathering the reactions mainly based on hydroxyl radical ( $\text{HO}^\bullet$ ) chemistry, which is the major reactive intermediate responsible for organic substrate oxidation. With photocatalysis, the AOTs also include ozonation, photo-Fenton, and  $\text{H}_2\text{O}_2$  reactions [1]. The complete list, given by Bhatkhande et al. [2], of organic molecules photooxidized by  $\text{TiO}_2$  is very large and confirms photocatalysis as a very successful AOT.

However, photocatalysis can also be used in environmental chemistry for metal reduction, for example, in the case of  $\text{Cr}^{6+}$  reduction to  $\text{Cr}^{3+}$ ,  $\text{As}^{5+}$ , and  $\text{As}^{3+}$  reduction to  $\text{As}^0$ ,  $\text{Hg}^{2+}$ , and  $\text{Hg}^0$  [3], or  $\text{NO}_x$  and  $\text{SO}_x$  reduction.

Titanium dioxide is one of the most important semiconductors in the family of transition metal oxides. It is mainly used as a white pigment (in paint, plastics, papers, foods, pharmaceuticals) and as UV absorber in sunscreens. It has been widely investigated because of its attractive application in photovoltaic and photocatalysis. The process of photocatalysis used for purification of air and water has mainly developed around the  $\text{TiO}_2$  due to significant advantages presented by this compound: chemical stability, non-toxicity, low cost, abundant natural resources, and ability to degrade a wide range of both gaseous and liquid pollutants. Indeed, the energy levels of  $\text{TiO}_2$  (VB and CB) are located in an adequate way compared to the redox potential of many organic species and those of water and oxygen. However, its large bandgap (around 3.2 eV), corresponding to an onset of the optical absorption band at about 380 nm, means that the photoactivity can be observed only under UV light excitation.

Numerous excellent reviews have been written in the field especially on the topic of photocatalysis for pollutant degradation [4–7]. This article is focused on the oxidative properties of  $\text{TiO}_2$ . The first part of this chapter is devoted to introduction of  $\text{TiO}_2$  and its photo-induced processes (Sects. 6.1, 6.2 and 6.3), after which we treat photocatalytic reaction and mechanisms (Sect. 6.4) in detail. The next two parts describe the benefit of the photocatalysis in environmental chemistry (Sect. 6.5) and examples of reactors used for wastewater treatment are described for illustrative purposes (Sect. 6.6) and finally, conclusions are given in the last part (Sect. 6.7).

**Table 6.1** Crystallographic data of different TiO<sub>2</sub> polymorphs

	Rutile	Anatase	Brookite
Crystallographic structure	Tetragonal	Tetragonal	Orthorhombic
Space group	P4 <sub>2</sub> /mnm	I4 <sub>1</sub> /amd	Pcab
Cell parameters (Å)	a = 4,5933 b = – c = 2,9592	a = 3,7852 b = – c = 9,5139	a = 9,1819 b = 4,4558 c = 5,1429
Z (molecules/cell)	2	4	8
Structure			
Ti coordination	6	6	6
Density	4,24	3,83	4,17
Ti–O distances (Å)	2 at 1,946 4 at 1,984	2 at 1,937 4 at 1,964	2 at 1,993 1 at 1,865 1 at 1,919 1 at 1,945 1 at 2,040

## 6.2 General Aspects

### 6.2.1 Crystalline Structure

Three polymorphs of titanium are mainly observed, rutile (thermodynamic phase), anatase, and brookite (metastable phases). All structures are built-up of TiO<sub>6</sub> octahedra but differ in their stacking. Rutile crystallizes in the tetragonal system (space group P4<sub>2</sub>/mnm) [8]. The structure can be described as arrays of linear chains of edge-sharing octahedra along the *z*-direction and the connection between these channels is through the sharing of vertices in both directions *x* and *y*. Anatase crystallizes in the tetragonal system (space group I4<sub>1</sub>/amd) [8]. The structure can be described also as arrays of zigzag chains of octahedra linked by edges and each octahedron shares four edges. Brookite crystallizes in the orthorhombic system (space group Pcab) [9]. Its structure can be described as arrays of zigzag chains of octahedra sharing three edges. These chains are plans in the *x* and *z* and the connection between these plans is done along the *y* direction by sharing vertices. Their structures are shown in Table 6.1.

Brookite possesses a more distorted structure than anatase or rutile as it has only two Ti–O bonds of identical length. These dissimilarities may involve differences in reactivity at the particle surface as well as in the redox level. Similarly, rutile possesses a more compact structure than the other two, which can also have consequences on its reactivity.

### 6.2.2 Electronic and Optical Properties of $\text{TiO}_2$

Being the thermodynamic phase, rutile is stable under thermal treatment while anatase and brookite undergo a non-reversible phase transition into rutile when heated at high temperature. At nanoscale, it was reported that the transformation sequence among the three  $\text{TiO}_2$  phases is dependent on size of the particle ( $d$ ) and pH. Indeed, the energies of the three phases are sufficiently close to one another to be reversed by small differences in surface energy. Anatase is thermodynamically most stable when  $d < 11$  nm, brookite is the most stable phase when for  $11 < d < 35$  nm, and while  $d > 35$  nm, rutile is the most stable phase [10]. However, rutile is stabilized relative to anatase in very acidic solutions, whereas in very alkaline solutions anatase is stabilized relative to rutile and brookite [11].

The electronic properties of the  $\text{TiO}_2$  vary according to the studied polymorph as describe in detail later. Detailed studies on rutile at low temperatures showed that the bandgap near the edge is dominated by direct transitions at 3.06 eV (405 nm,  $T = 1.6$  K) [12–15]. In the case of anatase there is a consensus that the absorption edge is around 3.2 eV (384 nm), associated with indirect transitions [16, 17]. Brookite has bandgap energies ranging from 3.1 to 3.4 eV (365–400 nm), both smaller and larger than the anatase one, and there appears to be no consensus on whether direct or indirect transitions dominate the optical response [18–21]. These values give transitions in the ultraviolet domain. Due to lower size the bandgap of  $\text{TiO}_2$  particles at the nanoscale are larger than the bandgap of bulk  $\text{TiO}_2$  [18, 22–25]. For example, the lower edge of the CB for nanosheet is approximately 0.1 V higher, while the upper edge of the VB is 0.5 V lower than bulk anatase [23].

### 6.2.3 Synthesis of $\text{TiO}_2$

The synthesis of nanostructured  $\text{TiO}_2$  (nanoparticles, thin films, nanoporous materials) is available, thanks to the variety of preparation methods: mechanical, chemical, or physical; in liquid or gas medium.

Rutile is mainly prepared by hydrothermal approach (relatively high temperature and pressure). Indeed, the rutile phase is thermodynamically stable and its formation needs “hard” conditions such as acidic media, high temperatures, and/or long aging time [26–30]. Nanorutile can, nonetheless, be obtained by soft chemistry [31–34]. Synthesis routes of anatase are numerous and varied because of its metastability. The hydrothermal syntheses are frequently employed in the literature, but the hydrolysis of Ti(IV) precursors under mild conditions is the most widely used method, sometimes through the intermediary of a gel [35, 36]. The precipitation in aqueous solution is also reported [34]. Some works refer to other ways of syntheses [37–39]. Brookite phase is still an exotic phase and few works report the synthesis of pure brookite especially at the nanoscale. Indeed, the most common synthesis routes are hydrothermal ways but they lead essentially to micrometer-sized particles [19, 40–45]. The

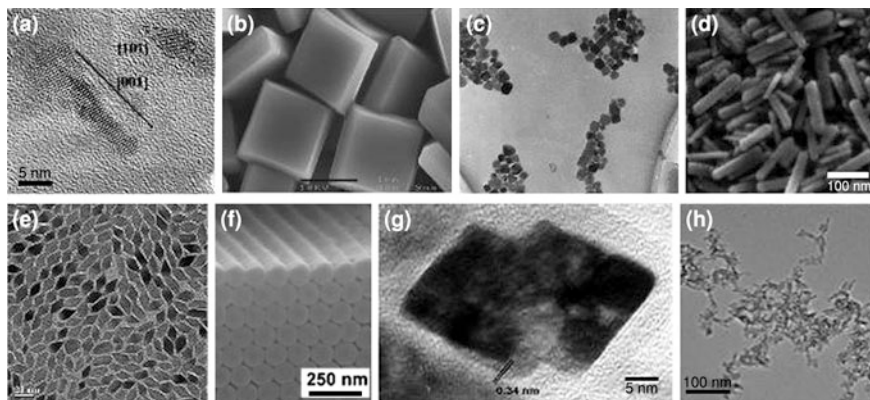


**Fig. 6.1** Particle morphologies of nanosized  $\text{TiO}_2$  for **a–f** Anatase, **g** Brookite, and **h** Rutile. For synthesis methods and details: **a** [49], **b** [50], **c** [36], **d** [51], **e** [52], **f** [53], **g** [48], **h** [31]

nanometric brookite can be synthesized by thermohydrolysis of  $\text{TiCl}_4$  in aqueous media [20, 32, 46–48]. Depending on synthesis conditions the observed morphologies are highly various, even for a same crystalline structure (Fig. 6.1).

### 6.2.3.1 Sol–Gel Synthesis

It is a versatile synthesis and a low-cost process. In the case of  $\text{TiO}_2$ , it consists of hydrolysis of a titanium precursor [Ti(IV) alkoxide or a salt] followed by condensation at low temperature leading to the inorganic framework. In aqueous solution, a colloidal suspension is then formed (the sol) and depending on the synthesis conditions (pH, concentration, acidity, temperature, etc.), anatase, rutile, or brookite phases can be synthesized with a fine control of size and morphology of the particles. In alcoholic medium, one can observe a transition to gel after loss of solvent and total polymerization. By adjusting the reaction conditions (pH, solvent, additives), it is possible to design the nanoparticles obtained.

Many nanostructures can be formed by sol–gel methods: size and shape controlled nanoparticles [54, 55], nanocubes [36, 56], nanorods [57], and nanowires [58]. Thin films can also be obtained by coating the sol onto various substrates by dip-coating or spin-coating. Porous materials (meso- or nanoporous) are widely studied since the specific area of the materials is considerably increased. The use of surfactant is often described, which allows, in some cases, the formation of a template during the synthesis [59, 60].

The advantages of this method are the purity of products, the homogeneity, the flexibility, the ease of implementation, the possibility of introducing dopants in high concentration, and its easy use to make thin films on surfaces.

The methods of micelles and reverse micelles can also be cited for the formation of well-controlled nanosized particles [61, 62].

### 6.2.3.2 Hydro- and Solvothermal Synthesis

These methods involve chemical reactions of a titanium precursor in aqueous (hydrothermal method) or organic solvent (solvothermal method), at controlled temperature and pressure. The temperature may approach the boiling water temperature in hydrothermal method and thus the saturation vapor pressure, or may be much higher for the solvothermal method where a solvent with high boiling point is used. These techniques allow obtaining nanoparticles, small size distribution, and controlled crystallinity by adjusting the experimental conditions. Nanowires, nanotubes, or nanorods can also be synthesized by these methods [63–65]. Finally, other synthesis approaches, not really in liquid media but rather in a supercritical fluid, have been studied [66].

### 6.2.3.3 Direct Oxidation and Electrodeposition

The direct oxidation of titanium consists of chemical or anodic oxidation of titanium metal [53, 67, 68] and leads to the formation of TiO<sub>2</sub> nanorods or nanotubes.

As for electrodeposition, it is a technique used to produce surface coatings. The substrate plays the role of cathode and is immersed in a solution of precursor salts of the material to be deposited. By adjusting the parameters such as the electrolyte, the working potential, the current density, the temperature, and the pH, it is possible to control the structure and morphology of the deposit. TiO<sub>2</sub> nanoparticles could be deposited on various substrates such as carbon nanotubes [69].

### 6.2.3.4 Chemical Vapor Deposition

It involves a chemical reaction during which a precursor in vapor phase is condensed to form a solid-phase material. This process that can be used in a flow production is employed to form coatings on many substrates, films, and fibers or to develop composite materials by infiltration [70]. Thus thin films of TiO<sub>2</sub> with controlled grain size, nanoparticles, or nanorods have been synthesized [71, 72].

### 6.2.3.5 Mechanochemistry

This technique consists of grinding the micrometric powders by action of ceramic balls under strong agitation. The material is then crushed until a nanosized powder is obtained. The mechanochemical synthesis, where the nanopowder is formed by a chemical reaction induced by mechanical grinding [73] is also used.

## 6.2.4 Influence of Some Parameters on Photocatalytic Efficiency

Photocatalytic activity is dependent on the surface and structure properties of the semiconductor such as crystal structure, surface area, particles size, porosity, bandgap, and surface hydroxyl density. Despite a huge number of publications in which TiO<sub>2</sub> nanoparticles with different crystalline phase, size, and morphology were studied in terms of photocatalytic activity, the relationships between morphological and structural properties and the catalytic behavior still remain unclear.

### 6.2.4.1 Crystalline Structure Effect

Anatase, brookite, and rutile TiO<sub>2</sub> have a photocatalytic activity [74]. It was shown that anatase was the most active [75, 76]. Indeed, the potential of the CB is more negative for anatase and for rutile, which promotes the reduction of oxygen and thus reducing recombination, making more efficient anatase form [77]. It also seems that other parameters are involved, as the mobility of charges created in the matrix of the semiconductor TiO<sub>2</sub> under the effect of photons. Work on the comparison of the photoconductivity of the anatase and rutile has shown that the lifetime of charge carriers is higher for anatase than for rutile [78, 79]. In addition, the rate of recombination is significantly higher for rutile. This recombination slows down the photodegradation of pollutants because it prevents the formation of oxidizing species, mandatory for the mineralization of organic matter adsorbed on the surface of grains.

Mainly because of the difficulties encountered in its synthesis, phase-pure brookite has been significantly less characterized as compared to anatase or rutile but good photoactivity is reported in the literature [44, 80–82]. For example, brookite nanoplates exhibit higher efficiency than rutile and anatase in the bleaching of methyl orange solution under UV irradiation [51, 83, 84].

Although the anatase phase usually has a better photocatalytic activity than brookite and rutile, the mixture of anatase and rutile in the *Evonik* P25 material (~80 % of anatase and 20 % of rutile) demonstrated extraordinary photocatalytic activity. It has become a reference for photocatalytic tests. The series of PCX anatase from *Cristal Global* (X refers to the specific surface, it decreases with the increasing sintering temperature) and *Hombikat* UV-100 from *Sachtleben* are also frequently used and compared with various synthesized materials. The characteristics of the reference powders are given in Table 6.2

The good photocatalytic activity of *Evonik* P25 was reported to be due to slowed down recombination between electrons and holes. It was postulated that the smaller bandgap of rutile absorbs the photons and generates electron–hole pairs. The electron transfer takes place from the rutile CB to electron traps in the anatase phase [85]. Concerning the *Hombikat* UV-100 it was reported that the high photoactivity is due to the fast interfacial electron transfer rate [86].



**Table 6.2** Characteristics of the PCX series P25 and UV100

Sample	Phase composition (%)	Crystallite size (nm)	S <sub>BET</sub> (m <sup>2</sup> g <sup>-1</sup> )	Mean pore diameter (nm)
PC10	Anatase 100	65–75	10	24.1
PC50	Anatase 100	20–30	54	20.1
PC105	Anatase 100	15–25	85–95	15.3
PC500	Anatase 100	5–10	317	6.1
P25	Anatase 79 Rutile 21	22	51	31.5
UV100	Anatase 100	13	289	<50

#### 6.2.4.2 Size Effect

The size of the particles of the catalyst is an important parameter for photocatalytic efficiency since higher initial surface sites is expected with the decrease in size [87]. However, the predominant pathway for electron–hole recombination may be different depending on the particles size, especially at the nanoscale, where the surface/volume ratio is very large. In 1984, Tsai and Chung [88] showed that the decomposition of CO increased as the radius of the particles decreased. According to the theoretical and experimental studies found in the literature it seems that there is an optimal value of the particles size around 10–20 nm. For example, Zhang et al. [89] have shown that a size of 10 nm was the most appropriate for the photodegradation of chloroform. This is actually a compromise between surface reaction and recombination of electron–hole pairs. Tomkiewicz [90] has written a review on the influence of particle size in photocatalysis. However, the optimal size rather depends on the photocatalyst used, the pollutant studied, as well as the reaction conditions.

Another parameter involved in the particle size effect is the crystallinity of the particles. Indeed, the quality of the semiconductor crystals free of defects will help to avoid the recombination of electron–hole pairs. It has been reported that the photocatalytic activity of amorphous TiO<sub>2</sub> is negligible showing the importance of crystallinity [91, 92]. Several studies have shown that the crystallinity is improved with the calcination of the particles leading to increased photocatalytic degradation efficiency; nonetheless, a prolonged calcination results in a reduced efficiency since the surface area of the catalyst decreases.

The surface area is also a key parameter, since photocatalysis occurs through a surface transfer and consequently, the higher the surface, the higher the reaction sites number. However, the surface represents a zone of defects, which are traps for the electron–hole pairs, if the surface area increases too much, increasing the number of defects can involve a too high rate of recombination. The relationship between physical properties and photocatalytic activity is complex. Structure and size of TiO<sub>2</sub> nanoparticles are significantly dependent on the calcination temperature [93]. Indeed, the temperature promotes phase transformation and a growth of the crystallites. Agrios and Pichat [94] have studied the effect of the sintering

temperature of the PCX photocatalysts on photodecomposition of phenol, anisole, and pyridine in water. They have shown that the sintering has two important effects: (i) decreasing the concentration of crystal defects and (ii) increasing the average particle size, i.e., lowering the surface area. This results in a decreased rate of recombination of photogenerated electrons and holes, and also in a sintering of small crystallites into larger agglomerates leading to a decrease in surface area. In the case of phenol, reaction rates increase in the order PC500 < PC105 < PC50 < PC10, that is, in order of increasing heating although PC10 has a 30-fold less surface area than PC500. These results show that, for removal of phenol (without adsorption on photocatalyst), the decrease in the electron–hole recombination rate outweighs the decrease in surface area. Pyridine degradation follows the opposite tendency; since pyridine mainly reacts on the TiO<sub>2</sub> surface, the importance of surface area is essential.

#### 6.2.4.3 Surfaces and Exposed Faces Effect

The nature of the surface of the nanoparticles of TiO<sub>2</sub> plays an important role in the photodegradation due to the presence of surface hydroxyl groups. Indeed, the OH groups can directly trap the photogenerated holes producing very reactive surface HO• [4]. In addition, the surface charge, depending on the protonation/deprotonation equilibrium of the OH groups, induces a modification of not only the adsorption of the pollutant but also the amount of HO• formed. That is why the pH of the reaction dramatically influences the efficiency of the photodegradation [95]. The isoelectric point (IEP) of TiO<sub>2</sub> is about 6 (6.25 for P25 for instance [96]), therefore interactions with cationic electron donors and acceptors will be favored at pH > IEP, while interactions with anionic electron donors and acceptors will be favored at pH < IEP. However, the difference in IEP values of various TiO<sub>2</sub> can affect the reaction mechanism; moreover specific interactions may occur between certain pollutants and selected surface sites.

In addition the pH value can modify the state of chemical species in solution, which is closely related not only to the dissociation constant but also to the adsorption mode of pollutants. It is thus important to study the nature of the TiO<sub>2</sub> particles and the pollutants to be degraded and determine the optimum pH.

The morphology of the photocatalysts is also reported to be an important parameter [97]. Under equilibrium conditions, anatase crystals are mainly octahedral bipyramids with {101} facets, which have the lowest energy rather than the more reactive {001} facets [52]. Recently, numerous studies have reported the preparation of anatase TiO<sub>2</sub> nanoparticles with higher energy surfaces [50, 98]. They successfully synthesized high-quality anatase TiO<sub>2</sub> crystals with exposed {001} facets. Their higher efficiency in the photocatalytic degradation of organic compounds is related to the predominance of {001} surfaces [99–103].

It has also been reported that the photocatalytic activity of TiO<sub>2</sub> nanotubes (synthesized from anodization of Ti) can be much higher than for TiO<sub>2</sub> nanoparticles [68]. The higher efficiency of the tubes (in spite of their lower surface

area) compared with P25 can be ascribed to (i) a more optimized geometry with significantly shorter carrier-diffusion paths in the tube walls (10–15 nm), including less trapping and recombination of electron–hole pairs (ii) a shorter diffusion path for pollutant molecules from the solution to the active surface area.

### 6.2.5 Improvements

The optical absorption of  $\text{TiO}_2$  is unable to use efficiently the whole solar light spectrum for photocatalysis since less than 5 % of the solar light energy can be absorbed by  $\text{TiO}_2$  while the visible part of the spectrum represents  $\sim 43$  % of total energy received. This explains the continuous interest in increasing the photoactivity under visible light. Three ways are studied: (i) the doping of  $\text{TiO}_2$  with metallic ions [104] or heteroelements [105] to change the gap by inserting new states in the bandgap, (ii) the sensitization by organic or inorganic dyes, which can improve optical activity in the visible region (not presented here) [106, 107], (iii) a third possibility is to modify the surface of  $\text{TiO}_2$  by pretreatment or by coating with other semiconductors [108] or metals to improve the charge transfer between  $\text{TiO}_2$  and the overall system.

#### 6.2.5.1 Doping

The syntheses are realized by wet chemistry (usually involving hydrolysis of a titanium precursor in a mixture of water and other reagents, followed by heating), high-temperature treatment, or ion implantation into  $\text{TiO}_2$  nanomaterials.

*Cation doping:* Different metals have been used to dope  $\text{TiO}_2$  by methods of wet chemistry [104], treatment at high temperature, or ion implantation [109]. In the literature doping with metal ions V, Cr, Mn, Fe, Co, Ni, Cu, Zr, Sn, W, etc., lanthanides La, Ce, Nd, etc., [110] or with alkali metals Li, Na, K [111] are found.

*Anion doping:*  $\text{TiO}_2$  has been doped with several hetero atoms: B, C, N, O, F, S, Cl, Br, by the three different methods. For example, hydrolysis of titanium tetra isopropoxide (TTIP) in a water/amine medium followed by treatment with amines [112] or high-temperature annealing of  $\text{TiO}_2$  under ammonia [113] or ion implantation under nitrogen [114] leads to a nitrogen-doped  $\text{TiO}_2$ .

#### 6.2.5.2 Surface Modification

*Surface treatment:* The surface can be modified by pretreatments such as sulfation, reduction with hydrogen, or halogenation. For example,  $\text{TiO}_2$  has been treated by  $\text{SO}_4^{2-}$  to form superacid solid, which shows an increased photoactivity in various organic reactions [115]. Sulfation of the catalyst leads to an increase of the surface

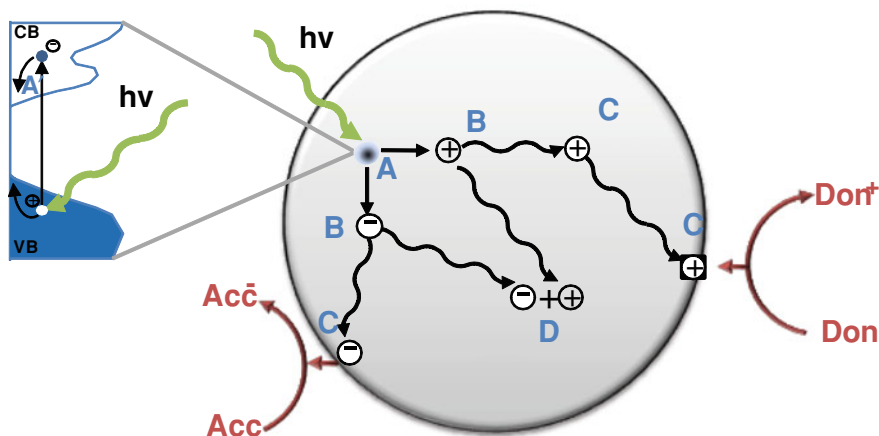


**Fig. 6.2** Schematized description of different steps of the photocatalytic process

acidity [116] and an increase of adsorption strength and therefore to an improvement of the adsorption coverage of the substrates.

Any materials with a narrower bandgap or absorption in the visible or infrared domain can be used to coat  $TiO_2$  materials.

*Sensitization by semiconductors:* The synthesis method is usually the sol–gel method and the sensitizers are numerous. We can find studies on  $CdS$ ,  $PbS$ ,  $Ag_2S$ ,  $Sb_2S_3$ , and  $Bi_2S_3$ ,  $AgI$ ,  $CdSe$ ,  $InP$ ,  $WO_3$ ,  $Fe_2O_3$ ,  $ZnO$ , and  $SnO_2$  [117–119].

*Metal coating:* Metal deposition on the  $TiO_2$  surface enhances photocatalytic reactions by accelerating the transfer of electrons to dissolved oxygen molecules. There is an optimum loading value above which metal deposition has a detrimental effect on the photocatalytic activity. Metals such as  $Pd$ ,  $Pt$ ,  $Ag$ ,  $Cu$  have been deposited on  $TiO_2$  particles, by sol–gel methods [120], mechanical mixing [121], chemical deposition, precipitation–reduction [122], and photodeposition.

## 6.3 Fundamental Aspects

### 6.3.1 Introduction

The entire photocatalysis process may be decomposed into several single steps occurring successively or simultaneously in the material, onto the surface or close to this surface. These different fundamental physical and chemical phenomena are summarized in the scheme displayed in Fig. 6.2.

The first step corresponds to the promotion of an electron from the VB to the empty CB (and thus the creation of a positive hole in the VB) induced by the uptake of a photon by the semiconductor. The generated charges (electron and

hole) are effectively separated and may then migrate, be trapped, or recombine. The charges that migrate or are trapped close to the surface may either be transferred to the electronic levels of the targeted surface adsorbate or generate radicals that allow remote photocatalysis reactions. Some of those events proceed in the time scale of the femtosecond hence requiring time-resolved experiments with high accuracy. Others happen more slowly but may not easily be studied, as no physical parameter is directly accessible experimentally. Consequently, these fundamental issues were only addressed in the last 30 years, especially in the last decade. The aim of this section is not to give a precise description of the state of the art in these fundamental domains, several recent reviews are available [123–128] and among them the very detailed review of the professor Henderson [129], but rather to draw an overview of the knowledge in the domain and the issues still in debate. The different aspects will be discussed in the order they occur in the whole catalytic process and the focus is put on the two main  $\text{TiO}_2$  structures anatase and rutile, the brookite phase being too scarcely obtained as pure materials to be extensively studied.

### 6.3.2 Photon Adsorption

The optical properties of the  $\text{TiO}_2$  structures are now experimentally well known and confirmed by theoretical calculations [130–132]. The lowest photon energies needed to promote an electron from the valence band to the conduction band are 3.2 and 3.0 eV for anatase and rutile, respectively, with an indirect bandgap in the former case and a direct one in the latter [130, 132]. However, when considering the energy levels in both bands displaying the highest density of states (i.e., the highest probability of transition) the transition is closer to 4 eV in energy. The light absorption coefficient increases exponentially with photon energy in the case of anatase while it is rather linear for rutile. When the photon energy used to promote the electron from the VB to the CB is much higher than the bandgap, the result is an electron in the CB significantly higher in energy than the bottom of the band or a hole generated not just below the top of the VB (cf Fig. 6.2) [133]. The bandgap values given for pure bulk materials at room temperature depend on various parameters listed and discussed below. Several of these parameters are used to tune the optical absorption domain of the materials and its efficiency.

First, a temperature increase was shown to decrease the optical absorption edge [133]. Moreover, the relative orientation of the anatase crystal toward the polarization direction of incident light was said to impact on the adsorption efficiency [133, 134]. However, this issue is still a matter of debate and the physical backgrounds are not clearly established. More important questions are raised by the use of nanoscale materials with a high surface/volume ratio that may alter the adsorptive properties. A geometric distortion of the  $\text{TiO}_2$  unit cells for very small particles may also have consequences. Indeed, a blueshift is observed for particles

smaller than 10 nm in size. This effect is even more pronounced in particles under 3 nm as confirmed by calculations [135, 136].

Surface modification by adsorbates and bulk doping are the two most used strategies to decrease the optical bandgap. The surface additives may be either organic such as dyes [137] and surfactants [138] or inorganic such as metallic ions and clusters [139, 140] or metal oxides [141]. For bulk doping of TiO<sub>2</sub>, the most studied route is an *n*-type self-doping associated to the presence of Ti<sup>3+</sup> ions in the lattice. Thus, the bandgap is decreased of about 0.8 eV but the question whether the transition occurs only between localized states is still controversial [142, 143]. A variety of cation-doped TiO<sub>2</sub> samples were prepared and tested in photocatalysis. Indeed, depending on the nature of the cation, the dopant creates additional energy states either at the bottom of the VB (with Fe) or at the top of the CB (with V) [144]. However, the presence of the cations in the lattice is not benign since some of the additives increase the charge carriers' lifetime while others decrease it [145]. The doping with anions was much more studied since the first demonstration of the photocatalytic activity of nitrogen-doped TiO<sub>2</sub> under visible light in 2001 [105], and the majority of the studies are focused on this element. The influence of the preparation mode and of the localization of nitrogen in the structure on the photocatalytic activity was extensively discussed [146]. The doping significantly decreases the UV activity of TiO<sub>2</sub> in comparison with the pure material because it favors recombination of charge carriers but it allows photocatalysis by visible light [147].

### 6.3.3 Charge Carriers Migration and Trapping

Once the electron is promoted into the CB it is still physically in the vicinity of the created hole and the charge carriers' pair is called an exciton. The stability of the charge pair is due to the mutual attractive electrostatic interaction, which may be hampered by the high dielectric constant of TiO<sub>2</sub>. Its destiny is almost always seen as the evolution (migration, trapping) of separated holes and electrons. Indeed, very few is known about the way the excitonic state may be trapped or migrate while it is known that the charge separation may not occur immediately [130, 133].

When electrons and holes are not trapped in an excitonic state or do not recombine (cf. below) they may migrate in the solid. In parallel to that migration, the charge carriers will 'thermalize', that is to say reach their lowest energy state at the edges of the bandgap. This thermalization is quite fast for 'hot' electrons, in the range of the 100 fs time scale [148] and longer for 'hot' holes (up to 100 ps) so those carriers may reach the surface without being totally thermalized [149]. As for charge transport in a semiconductor, mobility may be seen for both carriers as a succession of hopping from one lattice site to another [150, 151]. Some sites (especially those close to the surface) that correspond to deeper surface potential wells are able to stop the charge migration for a certain duration and are consequently considered as trapping sites. Electron transport is strongly promoted by

electron–phonon coupling, and as a consequence, is said to be anisotropically efficient [150–152]. The Marcus theory for polaron hopping was then efficiently used for bulk anatase and rutile systems. Differences between the two structures and between two different directions in the same structure were observed [153]. The hole transport phenomenon is less understood as the interactions with phonons seem to be less effective.

An important issue in the lifetime of charge carriers concerns their trapping in specific sites. This trapping may be seen as an undesired event if it prevents the charges to reach the surface but may also be considered as favorable if it facilitates charge separation or if the charges are trapped close enough to the surface to react. Most of the electrons are believed to be trapped close to the surface but the precise location is matter of debate for some studies propose an electron trapping on subsurface Ti sites while others studies locate it on under coordinated Ti located at the surface [154, 155]. However, the exact localization is not easy to determine for no experimental probe is able to address this issue. The amount of trapped electron is generally in the range of one trapped electron per nanoparticle [156]. The trapping of electron is very fast (shorter than 100 fs) while the trapping lifetime is at least in the picoseconds scale and may last several months if no electron scavenger is present [156, 157].

The hole trapping is much more difficult to study than the electron one and few quantitative results are available. EPR studies indicate that trapped holes are localized on negatively charged under coordinated surface oxygen sites [158]. Holes may be trapped as fast as electrons and the trapping lifetime may be equally long.

### ***6.3.4 Charges Recombination or Transfer on a Surface Adsorbate***

The charge recombination is the undesired fate of  $e^-/h^+$  pairs since the photo-converted energy is lost either through a radiative or more often a non-radiative way. Consequently, the measurement of the amount of recombination is of paramount importance to determine the efficiency of a photocatalyst. Some studies used the amount of mobile charge carriers to estimate the recombination rate [159, 160] while others used the consequences of the recombination such as the emitted photons or the heat generated [161, 162]. The photoluminescence due to radiative recombination also gives information about the trapping sites and the carrier thermalization. The charge recombination kinetic and intensity strongly depend on materials characteristics and especially its crystallinity [163]. Photons are mainly absorbed in the bulk and recombination most often happens between ‘free’ holes and electrons trapped at the surface. It was shown that for 2 nm anatase particles 78 % of the excitation events led to recombination after 20 ps while only 17 % in 27 nm particles [164]. More generally, half of the excitons are believed to be recombined in  $\text{TiO}_2$  in the tenths of nanoseconds time scale.

In order to play its role the charge must be transferred on a surface acceptor (*A*) or donor (*D*) that may be the final target compound of the photocatalysis, or may be simply involved in the catalytic process or only serve as a charge scavenger. Formally, the acceptor or donor may also be another solid with a band structure.

The electrons generated in  $\text{TiO}_2$  may be transferred in an empty energy state of the acceptor on the condition that the targeted state is below that of the edge of the CB or more precisely below the energy level of the trapped electrons. This electron transfer which corresponds to the starting point of a photoreduction mechanism demands a strong coupling between the energy levels in order to avoid electron back-transfer. Studies on the electron transfer on methyl viologen by UV-Visible time-resolved spectroscopy indicate that the electron is transferred in the picoseconds to nanosecond time scales [165]. In order to improve the quality of  $\text{TiO}_2$  for photooxidation, it is very important to improve the electron transfer to a scavenger that will prevent them to recombine with the photogenerated holes.

The photooxidation itself requires the electron transfer from a donor to  $\text{TiO}_2$  VB hole. Again, the relative position of the energy level of the donor and that of the edge of the VB is of peculiar importance. The good coupling between the two levels is also important. Indeed, a study showed that adsorbed alcohols (methanol and isopropanol) trap the hole in their vicinity to promote the charge recombination rather than transferring an electron into the VB [166]. Kinetic studies using  $\text{SCN}^-$  probe as a model adsorbate for hole transfer demonstrated that the transfer is done in the same time scale as that of electron one from the CB [167]. A paradox is raised here since a hole transfer process is said to be quite fast and efficient while photooxidation is usually said to be slow and inefficient. This last assertion is explained by the fact that the photooxidation of a molecule often involves multiple hole transfers with adsorbate that display different energy states and configuration. Hence all the steps are not equally fast and the global process is slow.

The charge transfer is the final step of the photocatalytic process with the  $\text{TiO}_2$  material and the next steps may be seen as the photodegradation mechanisms with a molecular approach. However, these mechanisms are truly photocatalyst dependent since the efficiency of the transferred electrons and holes depends on their pristine energy levels. In the case of radical-mediated mechanisms (as described below) the nature and amount of these radicals strongly depends on the used semiconductor. That is why the next section focuses first on the generation of radicals in the reactive medium and then on the direct photooxidation of organic molecules on the  $\text{TiO}_2$  surface.

## 6.4 Mechanisms

### 6.4.1 Generalities on Photooxidation on $\text{TiO}_2$

A large amount of studies try to elucidate the whole degradation mechanism of various organic and inorganic pollutants but the goal of this section is more focused on the mono-electronic events in which the  $\text{TiO}_2$  phase plays a role.



Besides the direct transfer of charges between the semiconductor and adsorbed targeted molecules, titanium dioxide may activate the solvent in order to generate radicals in solution such as  $\text{OH}^\bullet$  radicals. In aqueous solution and in a solid–gas reaction intermediate molecules such as oxygen may also create active radicals. These generated radicals are likely to react far from the photocatalyst and yet their nature and amount may be specific to the material used. Indeed,  $\text{TiO}_2$  is able to generate  $\text{O}_2^-$  ions while it is not the case for photocatalysts such as  $\text{Bi}_2\text{WO}_6$ . The observed degradation mechanisms are also dependent on the ability of the material to photoadsorb and photodesorb species that promote or inhibit the process [168]. For instance, the photodesorption of a product is interesting while the photoadsorption of an inert molecule may consume a useful charge carrier and block a reactive site at the surface of the material.

This section is mostly devoted to photooxidation of organic molecules but in non-photoelectrochemical settings the associated photoreduction process must happen in close vicinity. Consequently, the presence of electron scavengers are required to obtain good efficient photocatalysis conditions and knowledge about them is summarized below. Oxygen is the most used and studied electron scavenger but it plays different roles that are not yet fully understood. This molecule may be simply physisorbed on regular and fully oxidized surfaces while  $\text{O}_2$  dissociative adsorption proceeds on defective surfaces (oxygen vacancies) or on regular surface sites where electron transfer may easily occur via subsurface  $\text{Ti}^{3+}$  [169]. The species generated from  $\text{O}_2$  adsorption and charge transfer are more diverse when performed on hydroxylated surfaces and in the presence of water molecules:  $\text{HO}_2$  and  $\text{H}_2\text{O}_2$  species could be the observed near to the surface. In addition to thermal adsorption,  $\text{O}_2$  may also be photoadsorbed forming directly  $\text{O}_2^-$  species that rapidly evolve into  $\text{O}_3^-$  or  $\text{O}_2^{2-}$  in addition to the already quoted  $\text{HO}_2^\bullet$  and  $\text{H}_2\text{O}_2$  species. The electron transfer process on  $\text{O}_2$  often regulates the kinetics of the whole reaction process. Two additional electron scavengers proposed in the literature are  $\text{Fe}^{3+}$  ions in aqueous solution [170] and  $\text{NO}$  in the gas phase [171] but even if their role of scavenger is similar, the so-generated species do not play as an important role in the photodegradation mechanism as oxygen-derived species.

### 6.4.2 Photooxidation of Alcohols, Aldehydes, and Ketones

The photodegradation of alcohols was extensively studied and especially that of methanol and ethanol for they are model molecules for alcohols with longer chains and constitute intermediate in other photodegradation mechanisms. The photooxidation of methanol may follow both direct and indirect processes depending on the amount of water and oxygen present. Formate and formaldehyde intermediates were detected but the attribution of an intermediate to one or the other process is still controversial [172, 173]. Additional intermediates could be detected with low temperature (1.9 K) EPR study such as  $\text{CH}_2\text{OH}^\bullet$  and  $\text{CHO}^\bullet$  [174]. The temporal scheme of the different mechanistic steps is up to now not well established.

Similar to methanol, intermediate species observed with ethanol are acetaldehyde and acetate but formate is also detected [175]. The question of reactants/products surface coverage also has its importance since formed carboxylates are able to block the access of O<sub>2</sub> to the surface and consequently the photodegradation of ethanol. Accordingly, other studies indicated that the first step of ethanol degradation involves O<sub>2</sub><sup>-</sup> ions [176].

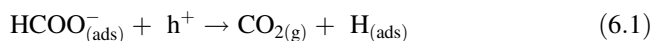
Another compound frequently used in photodegradation tests is phenol while relatively few studies are devoted to mechanistic details [177]. The first oxidation steps correspond to a hydroxylation on the aromatic ring involving OHHO• radical rather than a direct hole-mediated oxidation. However, the adsorption mode of phenol prior to oxidation remains unknown.

Among aldehydes, acetaldehyde was the most studied and was shown to transform into acetate. EPR studies of the reaction revealed a CH<sub>3</sub>C(O)OOHO• radical intermediate indicating the attack of O<sub>2</sub><sup>-</sup> on the adsorbed aldehyde [178]. Formaldehyde degradation mechanism is hard to study since it is rapidly converted into CO<sub>2</sub>.

For ketones degradation, mechanistic studies mostly involved acetone which mainly adsorb on oxide surfaces via an oxygen lone pair. A low temperature EPR study detected the formation of CH<sub>3</sub>COCH<sub>2</sub>OOHO• during the first reaction steps and the authors proposed that its formation occurs by the reaction of O<sub>2</sub> on an unstable CH<sub>3</sub>COCH<sub>2</sub>HO• radical generated by a first hole-mediated reaction [179]. The intermediates observed in another study are mainly acetate, formate, acetaldehyde, and formic acid corresponding to a C–C bond cleavage [180].

### 6.4.3 Photooxidation of Carboxylic Acids

Carboxylic acids photodegradation was widely studied because these molecules are initially often present in the pollutants composition or they may be obtained as photodegradation products of other organic molecules (alcohols, aldehydes, etc.). Carboxylates generally strongly adsorb on TiO<sub>2</sub> surfaces. Their stability on the oxide surface and the good knowledge of their different adsorption modes make them very interesting systems to understand the photo-induced reactions. Formic acid was widely studied; nevertheless, the mechanism is still controversial. The question remains between a direct hole-mediated pathway also called photo-Kolbe reaction (1) or an indirect pathway implying a HOHO• radical attack (2) [181].



In any cases, no intermediate could be detected before the formation of CO<sub>2</sub> [175]. The addition of water or oxygen in a solid–gas phase system significantly increases the degradation rate [175].

Another model molecule is acetic acid that was studied both on single crystals [182] and on high surface area systems [183]. Similar to formate, acetate may be degraded via the direct and indirect pathways but additionally,  $\text{HO}^\bullet$  radicals may attack the C–H bond of the methyl group leading to the formation of  $^\bullet\text{CH}_2\text{COOH}$  radicals. The photo-Kolbe reaction on acetic acid (3) also yields  $^\bullet\text{CH}_3$  radicals and consequently by-products such as  $\text{CH}_4$  and  $\text{C}_2\text{H}_6$ . Carbon isotopic labeling of acetate revealed that carboxylate carbon is first released as  $\text{CO}_2$  while the release of the other carbon is delayed and proceed through the chain methoxy, formaldehyde, and formate [183]. A detailed study on different rutile single crystals demonstrated that the amount of the obtained products significantly vary with the nature of the surface sites [184]. For other linear carboxylic acids the photodecomposition is said to proceed through a cascade of photo-Kolbe reactions that shortens the carbon chain of one unit each time up to formate. The Kolbe reaction is often observed in the degradation pathway of the carboxylic acids, except for phenyl-containing systems such as benzoic acid where an OH addition to the phenyl ring is favored [185].

#### ***6.4.4 Photooxidation of Alkanes, Alkenes, and Halo Hydrocarbons***

The main point of the photooxidation of alkanes and alkenes is their relative inertness toward the oxide surface and consequently the first reaction step creates intermediates that are more likely to bind to the surface. The next two examples of alkane degradation well show the diversity of possible intermediates and products. Cyclohexane leads in a first photocatalytic step to cyclohexanol and cyclohexanone with no ring opening or double bond formation [186]. The same authors proposed that cyclohexanol is formed from the cyclohexyl radical (obtained by a hole-mediated reaction on cyclohexane) while the cyclohexanone formation requires the attack of  $\text{O}_2^-$  anion. In the case of methane, different studies have shown either the formation of methanol, formate, and even ethane through the coupling of methyl radicals [187, 188].

Aromatics represent somehow a particular class of alkenes and their reactivity is very interesting even though not fully understood. Benzene and polyaromatics first undergo a  $\text{HO}^\bullet$  attack on the aromatic cycle prior to any ring-opening event [189]. However, in the case of toluene, the oxidation of the methyl group is favored in comparison with that of the aromatic ring leading to benzyl alcohol and benzaldehyde as reaction intermediates. According to an EPR study, this selectivity for the methyl group is attributed to the attack of an  $\text{O}_2^-$  leading to the formation of the  $\text{C}_6\text{H}_5\text{-CH}_2\text{-OO}^\bullet$  radical [190].

In comparison to the reactivity of alkanes that of halocarbons is complicated because the C–X bond may easily be broken to generate  $\text{X}^\bullet$  radicals and the free radicals may create mechanistic pathways in parallel to those involving the charge

carriers. That is well exemplified by the family of  $C_1$  chlorocarbons  $CH_{4-x}Cl_x$  for which numerous intermediates and products were observed such as carbon monoxide and dioxide, non-chlorinated  $C_1$  compounds, chlorinated  $C_1$ , and species with more than one carbon. The formation of more chlorinated species is a good indicator of the presence of radical chain reactions [191]. An additional specificity of halocarbons is the ability of the halogens to replace in certain conditions the surface OH group and consequently to poison the surface or to prevent the total mineralization of reactants by creating more halogenated species. Consequently, the addition of water may help to displace the surface OH/X equilibrium and thus favors the complete photodegradation process.

#### ***6.4.5 Photooxidation of Nitrogen-Containing Molecules and Miscellaneous***

As reported in this review [123], the N-containing molecules are likely to be at the same time subject to photooxidation and photoreduction. The alkylamines are more reactive under their neutral form as the lone pair of nitrogen is said to react with the  $HO^\bullet$  radical leading to the formation of an aldehyde and a less substituted alkylamine. The fate of the nitrogen of those molecules is generally nitrites, nitrates, and ammonia whereas the generation of  $N_2$  results mainly of a non-photocatalytic reaction between  $NO_x$  and  $NH_2^\bullet$  [192].

In the phosphorous-containing molecules the P–C bond seems to be more stable against oxidation than the P–O–C links and the oxidized products (usually a phosphate) poison the catalyst surface. This can be avoided if the reaction is carried out in presence of water in order to hydrate the adsorbed species and help to remove them from the surface. The same behavior of surface poisoning may be observed for organosulfides that yield sulfate surface groups.

The multi-functional molecules such as polysubstituted aromatics, or amino acids and halogenated acids were also studied, the two main questions tackled being the priority order in the degradation of the different organic functions and the efficiency of a cooperative effect between the different functions. For instance, a study led on chlorophenol showed that, depending on the wave length of the incident light, the molecule could react by OH addition without  $Cl^-$  removal to form chlorocatechol or with  $Cl^-$  removal to form hydroquinone [193]. In the halogenated acids family, the carboxylate group interacts with  $TiO_2$  and a Kolbe reaction is first observed in most of the cases [194].

The present overview of the mechanistic aspects of photooxidation of organic species on  $TiO_2$  clearly demonstrates that various parameters impact on the kinetic pathway: the functional groups, the presence of oxygen, and the nature solvent that may interact with the catalyst surface. Moreover, the nature of the exposed  $TiO_2$  surface and the presence of surface defects may affect the reaction mechanism as well.

## 6.5 Photocatalysis in Environmental Chemistry

The environmental applications of photocatalysis with  $\text{TiO}_2$  are gathered in three categories: air treatment, water treatment, and self-cleaning surfaces. The three categories include several domains:

- Air treatment: indoor and outdoor air decontamination, Volatile Organic Compounds (VOCs) and Polycyclic Aromatic Hydrocarbons (PAHs) elimination, sterilization, deodorization, etc.
- Water treatment: industrial and municipal wastewater treatment, discoloration, decontamination and disinfection, recalcitrant Chemical Oxygen Demand (COD) degradation, etc.
- Self-cleaning surfaces: self-cleaning and self-sterilizing, windows, buildings, tiles, lighting, walls, paintings, and pavements.

All these applications are using photoactive  $\text{TiO}_2$ , mainly under anatase form, considered as the most active phase. The photocatalyst can be used as free or supported powder, or in thin film, depending on the application. The set photocatalyst/support will be called photocatalytic media.

From now on, the described systems will mainly focus on organic oxidation in water. It should be noted that the problems are rather similar in the cases of inorganic reduction in water (in spite of different photocatalytic mechanisms) or organic oxidation in air (in spite of different reactor design). The category of self-cleaning surfaces is more distant and will not be developed here.

To be used in an environment application like wastewater treatment, the photocatalytic media should be active enough to realize the reactions in a reasonable time. It means that its activity should be previously estimated. Today, standardized tests for photocatalytic media are still in debate, and there is no established and indisputable molecule to evaluate the photoactivity.

In water, colored molecules such as rhodamine B or methylene blue (MB) have been widely used because the kinetic of the photoreaction is relatively high and because of the visual effect procured by the discoloration. However, their use is now contested because the bleaching may be ambiguous and not only due to the photodegradation of the molecule. In the case of MB, in the absence of oxygen and in the presence of a sacrificial electron acceptor (SED), MB is photoreduced to its colorless leucoform, LMB, by the  $\text{TiO}_2$  photocatalyst. While prolonged irradiation leads to the eventual complete mineralization of the dye, the initial observed photobleaching of the dye is not necessarily due to the dye oxidation, especially if the reaction is carried out under conditions that favor the formation of LMB [195].

Phenol is one of the most employed test molecule. It has been proposed by Serpone et al. [196], in 1996, as standard test molecule, and presents some advantages:

- It does not undergo degradation by photolysis or catalysis.
- It presents an absorption band at 269 nm detectable by UV-Visible spectroscopy.

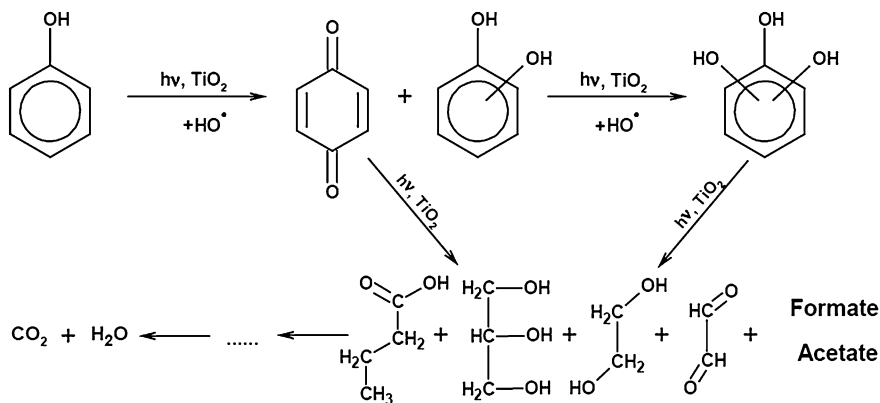


**Fig. 6.3** Proposed mechanism for phenol photodegradation on  $\text{TiO}_2$  [177]

- Its degradation mechanism is quite identified. The principal intermediates formed are benzoquinone, hydroquinone, and catechol. A mechanism is proposed in Fig. 6.3 [177].
- It follows a complete mineralization to  $\text{CO}_2$  and  $\text{H}_2\text{O}$ .
- It adsorbs very weakly at the surface of  $\text{TiO}_2$ .
- It is a real pollutant of water.

Other used test molecules are, for example, formic acid (mineralization without intermediates), stearic acid (model molecule for fat acids), 4-chlorophenol, trichloroethylene (model molecules for chlorinated compounds), and oxalic acid (molecule with adsorption on  $\text{TiO}_2$ ).

The test molecules are especially necessary for the setup of the reactor and for the elaboration of the photocatalyst, but to evaluate the performance of photocatalysis in water treatment, numerous studies are realized with real or model industrial wastewaters. It is quite difficult to compare these works with deeply different reactor design and photocatalytic media, but some interesting results may be pointed out. In most of these works, the problem is to evidence the degradation of the pollutant by photocatalysis, follow its kinetics, and analyze the eventual intermediates formation (intermediates may be more pollutant than the initial compounds). Photocatalysis is often presented as part of a general treatment process.

The next section presents recent obtained results of photocatalysis treatments on real industrial wastewaters, dyes, pesticides, antibiotics, and bacteria.

### 6.5.1 Real Industrial Wastewaters

The general objective of the study of Pichat et al. [197] was to evaluate under real conditions, in a parcel of vineyard, the practicability for the wine grower and the efficiency of a solar photocatalytic prototype device to treat rinse waters from tractor cisterns which are used to spray various mixtures of pesticides and

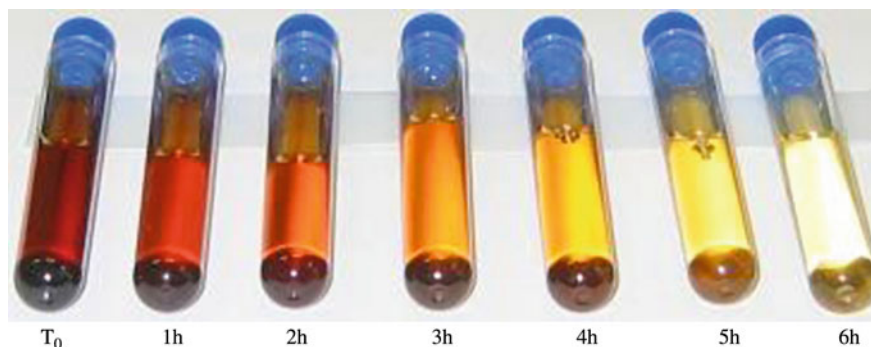


**Fig. 6.4** Discoloration of margins obtained by photocatalysis with  $\text{TiO}_2$  (photo Marjorie Mirau)

additives. This specific application of solar  $\text{TiO}_2$  photocatalysis shows promising results, although more on-site experimentations are required regarding its viability. Moreover, toxicity linked to inorganic ions remains a problem.

The photocatalytic treatment of an effluent from black table olive processing over  $\text{TiO}_2$  suspensions was investigated by Chatzisimeon et al. [198]. The study focused on the effect of various operating parameters on the treatment efficiency including initial organic load, catalyst type, concentration and reuse, and addition of hydrogen peroxide. Depending on the conditions employed, nearly complete discoloration was obtained, while mineralization never exceeded 50 %. Tests with non-acclimated activated sludge showed that both the original and photocatalyzed effluents were degradable aerobically. The biodegradation rate of the original effluent was three times greater than the oxidized one. On the other hand, photocatalytic oxidation of the original effluent was at least two orders of magnitude faster than its biological oxidation to achieve comparable levels of degradation.

Figure 6.4 is an illustration of the discoloration of margins (olive production wastewater) obtained by photocatalysis with  $\text{TiO}_2$ .

Rodrigues et al. [199] have investigated the combined treatment of post-bleaching effluent from cellulose and paper industry. The effluent was first submitted to a coagulation–flocculation treatment applying  $\text{FeCl}_3$  as coagulating agent and chitosan as auxiliary. The aqueous soluble phase obtained from the first treatment was then submitted to a  $\text{UV/TiO}_2/\text{H}_2\text{O}_2$  system. This combined method resulted in a high biodegradability index, transparency, and absence of color and odor in the treated water, suggesting good water quality.

In the work of Alinsafi et al. [200], photocatalysis with  $\text{TiO}_2$  particles immobilized on a glass slide or on a non-woven glass fiber fabric has been applied to pure reactive dyes (azo and metal phthalocyanines) solutions as well as textile wastewater containing the same dyes under UV and solar irradiation. Discoloration of textile wastewater was in the range 21–74 % under solar irradiation, with good COD removal rate. These values are strongly dependent upon the fine chemical structure of the dyes and the global composition of the wastewater. The results are encouraging for textile

wastewater remediation. The increase of biodegradability is an additional positive factor, as it would improve the efficiency of a biological downstream treatment.

An alternative method for municipal wastewater treatment has been developed by Antoniadis et al. [201]. It is based on solar photocatalytic oxidation and natural processes. The system combines the synergetic action of homogeneous photocatalytic oxidation with surface flow constructed wetlands in order to utilize the high solar irradiation and the ability of the constructed wetlands to improve water quality through natural processes. The authors have presented the design, the development, and an experimental evaluation of the combined system. Experiments were conducted at laboratory scale using artificial as well as solar irradiation, for the treatment of both synthetic and cesspool wastewater. The data evaluation revealed that the combined system may effectively reduce the organic load and nutrients of wastewater, even in cases of great inflow variability, in terms of hydraulic and organic load, and thus may be a promising, competitive, and environmental friendly solution for wastewater treatment in the near future.

### 6.5.2 *Dyes*

The photocatalytic degradation of five various dyes has been investigated in  $\text{TiO}_2$ /UV aqueous suspensions by Lachheb et al. [202]. They have tried to determine the feasibility of such a degradation by varying the chemical structures like anthraquinonic (Alizarin S), or azoic (Crocein Orange G, Methyl Red, Congo Red), or heteropolyaromatic (Methylene Blue). In addition to a prompt removal of the colors,  $\text{TiO}_2$ /UV-based photocatalysis was simultaneously able to fully oxidize the dyes, with a complete mineralization of carbon into  $\text{CO}_2$ . Sulfur heteroatoms were converted into innocuous  $\text{SO}_4^{2-}$  ions. The mineralization of nitrogen was more complex. The results suggest that  $\text{TiO}_2$ /UV photocatalysis may be envisaged as a method for treatment of diluted colored wastewaters not only for discoloration, but also for detoxification.

Sauer et al. [203] proposed a detailed investigation of the adsorption and photocatalytic degradation of the Safira HEXL dye, an anionic azo dye of reactive class. The dye is easily degraded by a  $\text{TiO}_2$ -assisted method in aqueous dispersions under irradiation by UV light. The adsorption of the dye is a prerequisite for the degradation. Both adsorption and photodegradation occur more extensively when the pH is near the PZC.

Among all the works on dyes photodegradation, Basic Red 46 [204] and C.I. Reactive Orange 4 [205] have also been studied and a rapid discoloration of the compounds is evidenced.

### 6.5.3 *Pesticides*

Herrmann and Guillard [206] have studied the influence of the basic photocatalytic parameters on the catalyst activity as well as the identification of reaction intermediate products and degradation pathways in model and real solution,



encountered in agricultural areas (rinsing waters). Various pesticides intensively used in agriculture such as herbicides [2,4-D(dichloro-phenoxy-acetic acid)] or insecticides (tetrachlorvinphos, fenitrothion, pirimiphos-methyl, fenamiphos) were successfully degraded, either as pure active agents or as commercial formulated reactants.

Devipriya and Yesodharan [207] realized a complete and quite exhaustive review on pesticides degradation by photocatalysis, with special reference to the mechanism of the process involved, the nature of the reactive intermediates, and the final products. Pesticides, insecticides, fungicides, herbicides, and additives were taken into account.

#### 6.5.4 *Bacteria*

Guillard et al. [208] presented a fundamental research on the efficiency of photocatalysis in water disinfection. Two model strains of *Escherichia coli* were selected and a comparison of the efficiencies of TiO<sub>2</sub> Evonik P25 versus TiO<sub>2</sub> Cristal Global PC500 was estimated. This work clearly pointed out the important difference with the photocatalytic removal of organic molecules. One has to take into account the size of the microorganisms compared to those of semiconductor and of organic molecules. The efficiencies of TiO<sub>2</sub> Evonik P25 on the inactivation of *E. coli* strains were comparable, whereas a more important inactivation of one of the strain of *E. coli* was obtained on TiO<sub>2</sub> Cristal Global PC500.

More recently, Pigeot-Rémy et al. [209] also studied the effect of Evonik P25 on *E. coli*.

In the study of Rizzo [210] the potential application of TiO<sub>2</sub> photocatalysis as primary disinfection system of drinking water was investigated in terms of coliform bacteria inactivation and injury. As model water, the effluent of biological denitrification unit for nitrate removal from groundwater, which is characterized by high organic matter and bacteria release, was used. Photocatalysis was effective in coliform bacteria inactivation, although no total removal was observed after 60 min irradiation time. Photocatalysis process did not result in any irreversible injury under investigated conditions, thus a bacteria regrowth may take place under optimum environment conditions if any final disinfection process (e.g., chlorine or chlorine dioxide) is not used.

#### 6.5.5 *Antibiotics*

In the study realized by Rizzo et al. [211], the degradation kinetics and mineralization of diclofenac (DCF) by photocatalysis on TiO<sub>2</sub> were investigated in terms of UV absorbance and COD measurements for a wide range of initial DCF concentrations and photocatalyst loadings in a batch reactor system.

TiO<sub>2</sub> photocatalysis was found to be very efficient for the mineralization, degradation, and detoxification of DCF, using low TiO<sub>2</sub> doses at achievable half-life time as well as using a lower potential lamp than previous studies.

In the work presented by Giraldo et al. [212], a photocatalytic system using titanium *Evonik* P25 in suspension was used to evaluate the degradation of antibiotic oxolinic acid (OA). The effects of catalyst load and pH were evaluated and optimized. The results indicated that TiO<sub>2</sub> photocatalysis allows a rapid and efficient removal of OA; transforming the initial substrate into by-products with no antimicrobial activity and lower toxicity, which could then be degraded in a subsequent biological step.

Degradation of amoxicillin, ampicillin, and cloxacillin antibiotics in aqueous solution by TiO<sub>2</sub> photocatalysis under UVA (365 nm) irradiation have been studied by Elmolla and Chaudhuri [213]. Enhancement of photocatalysis by addition of H<sub>2</sub>O<sub>2</sub> was also evaluated. The influence of pH on antibiotic degradation is evidenced. Kinetics of degradation was characterized.

## 6.6 Photocatalytic Reactors

The photocatalytic properties of TiO<sub>2</sub> described previously allow the development of wastewater treatment processes. For this purpose, a photocatalytic reactor must be designed. The photocatalytic reactors are different from classical ones (thermal or thermocatalytic) because of the irradiation, which activates the catalyst. The role of the reactor is to place simultaneously in contact the wastewater, oxygen, the UV illumination, and the photocatalyst. The photocatalytic reactor design implies taking into account parameters like the immobilization and the irradiation of the photocatalyst, the flow and the concentration of the wastewater and the oxygen, the cooling and the protection of the lamp, and the electric circuit. The final proposed design of the photocatalytic reactor will depend on those parameters.

In the photoreactor, the photocatalytic powder should be in close contact with the effluent. To avoid filtration difficulties, an immobilization of the photocatalyst is necessary. Depending on the design, it can be realized on glass beads or plates, sand, steel, or structuring porous materials (silica, zeolites, active carbon, carbon nanotubes, and nanorods). As demonstrated in the previous section, the sol-gel method allows the synthesis of a photocatalytic film or deposit [214]. Besides, the Ahlstrom Company produces a paper with deposited TiO<sub>2</sub> usable as flexible photocatalytic media [215]. It must be noted that, whatever is the support, the immobilization lowers the photoactivity because part of the solid is no more reachable to the UV photons.

The illumination producing photocatalysis may be provided artificially by a UV lamp or naturally by the sun.

In the case of the sun illumination, because of the weak intensity of the UV usable radiation, the illuminated surface and the photocatalyst/water contact surface must be high. The main questions are getting around photocatalyst



**Fig. 6.5** Compound Parabolic Collecting Reactor (CPCR) at the Plataforma Solar de Almería (PSA) [218]

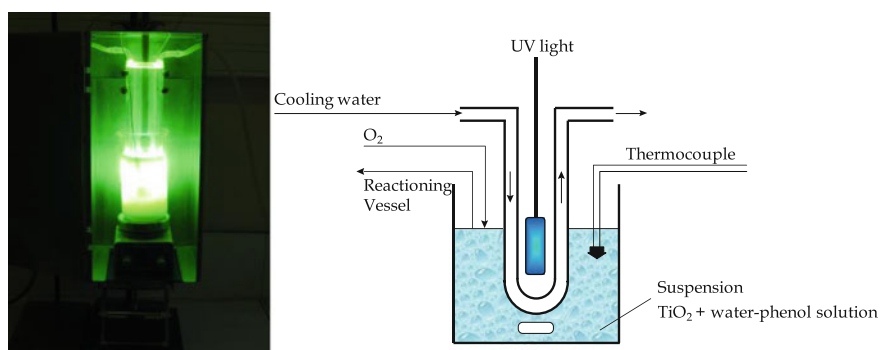


**Fig. 6.6** Batch reactor for photodegradation of phenol in water by  $\text{TiO}_2$

immobilization and sunlight concentration [216]. Different photoreactors have been developed Parabolic Trough Reactor (PTR), Thin Film Fixed Bed Reactor, Compound Parabolic Collecting Reactor (CPCR), Double Skin Sheet Reactor [216, 217]. Their design is different if they use solar concentrator and if the  $\text{TiO}_2$  is deposited or in suspension. PTR and CPCR are developed at the Platform a Solar of Almería located in the south of Spain, the place receiving the maximal sunshine of Europe (Fig. 6.5 [218]).

With artificial light, generally provided by one or several mercury lamp, the design is less restrained. Numerous examples are proposed [219]. The simplest model is the Batch Reactor allowing the illumination of a  $\text{TiO}_2$  suspension [4]. It is represented on Fig. 6.6. This kind of reactor, without immobilization of the

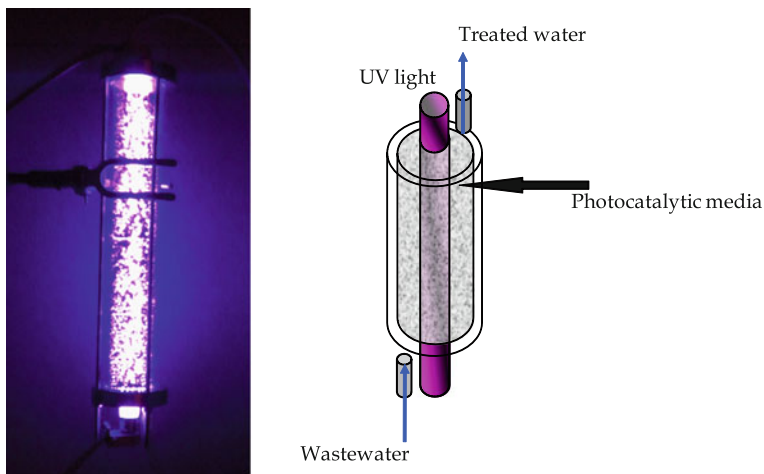


**Fig. 6.7** Annular reactor for wastewater treatment by photocatalysis

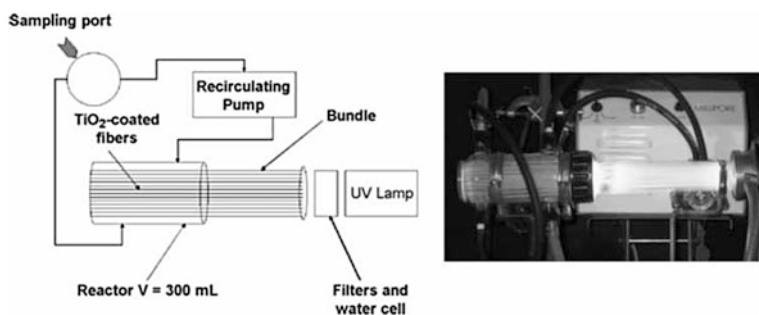


**Fig. 6.8** Photocatalytic reactor using optic fibers [226]

photocatalyst is mainly useful in the framework of photocatalytic tests for materials.

To avoid the filtration step, fluidized bed and fixed bed reactors are proposed. In the last case, an annular geometry represented in Fig. 6.7, with external or internal illumination, is often preferred [216].

Reactors with planar geometry are also described. More rarely, less classical systems are adopted (Rotating Drum Reactor [220], Intermittent Flow Reactor [219], Fiber Optic Cable Reactor [221, 222], Photocatalytic Membrane Reactor [223], Falling Film Photoreactor [224], Pulsed Baffled Tube Photoreactor [225], etc.).

Figure 6.8 from Danion et al. [226] shows a reactor using  $\text{TiO}_2$  deposited by sol-gel method on optical fibers.

Some processes use  $\text{TiO}_2$  monolith rather than an immobilized titanium dioxide but. Some systems are sometimes combining chemical, physical, or biological activity to the photoactivity [219].

The theoretical aspects of photocatalytic reactors have been mainly described by Cassano et al. [216, 227–229]. In this case, kinetic models of photodegradation including the simulation of the radiative field in the reactor are proposed for several geometries.

The radiation field inside photocatalytic reactors can be predicted by solving the radiative transfer equation (RTE). From the solution of the RTE, the local volumetric rate of photon absorption (LVRPA) can be obtained. This LVRPA is an important parameter in photocatalytic reactor design, energy efficiency assessments, and kinetic studies of photocatalytic reactions. However, to solve the RTE, optical parameters are needed: the absorption and scattering coefficients and the phase function. Solving the RTE may be arduous depending on the reactor geometry or the photocatalytic media.

In recent studies, the LVRPA has been evaluated in slurry using Monte Carlo techniques. In such simulated photocatalytic reactor, a photon is emitted from the lamp, travels a distance  $l$  and then is, according to a determined probability, either absorbed or scattered within the reacting medium [230].

## 6.7 Conclusions

The fact that an exponentially increasing number of articles are devoted to the synthesis of titanium dioxide nanoparticles and its application in photocatalysis is not surprising. It is indeed the reference material for that specific application and lots of authors evoke the possibility to improve the photoactivity to motivate their research. Moreover, various research domains still bring their contributions to the elaboration of the best photocatalyst possible for the whole process is quite complex and consequently very rich and diverse.

Indeed, a fruitful exchange occurred between physicists and material science chemists. While the former focus more on the fundamental aspects of the photocatalytic process from the photon interaction with the semiconductor up to the charge transfer to the reacting molecule, chemists are now tailoring very finely the nanoparticles in terms of composition, size, shape, and structure. A better understanding of the influence of each characteristic of a  $\text{TiO}_2$  powder on its photocatalytic efficiency is now possible but many fundamental issues are still under discussion.

A burning issue that involves both scientific communities is the question of how to use a higher amount of solar light to do photocatalysis. Each of the proposed solutions, such as bulk doping with nitrogen or heterostructures, presents drawbacks and hardly reaches the efficiency observed under UV light.

The capacity of  $\text{TiO}_2$  to photodegrade organic molecules via photooxidation was demonstrated from the simplest functional molecule of formic acid up to the scale of the bacteria. The understanding of each degradation step for the smaller molecules

may help in the future both to explain degradation of more complex ones and provide an interesting feedback to the elaboration of better TiO<sub>2</sub> photocatalyst.

A detailed study of the bibliography on degradation mechanisms of model organic molecules shows that certain experimental conditions such as the solvent, the bubbling of specific gas, or even the dispersion of the photocatalyst may favor the degradation of a molecule and block that of another. Consequently, the question of the definition of a good photocatalyst is very important and however very difficult to define. The need of normalized tests may emerge in a close future.

An important work is also devoted to preparation of reactors tuned to the desired decontamination process. The relative position of the light source, the photocatalyst, and the medium to be decontaminated must be carefully thought. Moreover, the global system must be scaled to reach the requirements of the decontamination efficiency and rate.

Finally, in every system where populations may use more or less directly the decontaminated fluids (air or water) a particular attention must be paid to the release of TiO<sub>2</sub> nanoparticles during the photodecontamination. Toxicology of TiO<sub>2</sub> nanoparticles is still under debate and numerous research projects are devoted to its toxicity as aerosols or in effluents. This is an especially important issue for all the people in laboratories and industries will have to handle this material that will surely be studied and used for the next decades.

## References

1. Gogate PR, Pandit AB (2004) *Adv Environ Res* 8(3–4):501–551
2. Bhatkhande D, Pangarkar VG, Beenackers AACM (2001) *J Chem Technol Biotechnol* 77(1):102–116
3. Litter MI (1999) *Appl Catal B* 23(2–3):89–114
4. Hoffmann MR, Martin ST, Choi W, Bahnemann DW (1995) *Chem Rev* 95:69–96
5. Carp O, Huisman CL, Reller A (2004) *Prog Solid State Chem* 32(1–2):33–177
6. Chen X, Mao SS (2007) *Chem Rev* 107(7):2891–2959
7. Fujishima A, Zhang X, Tryk DA (2008) *Surf Sci Rep* 63(12):515–582
8. Burdett JK, Hughbanks T, Miller GJ, Richardson JW, Smith JV (1987) *J Am Chem Soc* 109(12):3639–3646
9. Baur WH (1961) *Acta Crystallogr* 14(3):214–216
10. Zhang HZ, Banfield JF (1998) *J Mater Chem* 8(9):2073–2076
11. Finnegan MP, Zhang H, Banfield JF (2007) *J Phys Chem C* 111(5):1962–1968
12. Amtout A, Leonelli R (1995) *Phys Rev B Condens Matter* 51(11):6842–6851
13. Boschloo GK, Goossens A, Schoonman J (1997) *J Electrochem Soc* 144(4):1311–1317
14. Choi WY, Termin A, Hoffmann MR (1994) *Angew Chem Int Ed* 33(10):1091–1092
15. Pascual J, Camassel J, Mathieu H (1978) *Phys Rev B Condens Matter* 18(10):5606–5614
16. Asahi R, Taga Y, Mannstadt W, Freeman AJ (2000) *Phys Rev B Condens Matter* 61(11):7459–7465
17. Kavan L, Gratzel M, Gilbert SE, Klemenz C, Scheel HJ (1996) *J Am Chem Soc* 118(28):6716–6723
18. Koelsch M, Cassaignon S, Guillemoles JF et al (2002) *Thin Solid Films* 403:312–319
19. Li J-G, Ishigaki T, Sun X (2007) *J Phys Chem C* 111(13):4969–4976
20. Mattsson A, Osterlund L (2010) *J Phys Chem C* 114(33):14121–14132

21. Mo SD, Ching WY (1995) *Phys Rev B Condens Matter* 51(19):13023–13032
22. Monticone S, Tufeu R, Kanaev AV, Scolan E, Sanchez C (2000) *Appl Surf Sci* 162: 565–570
23. Sakai N, Ebina Y, Takada K, Sasaki T (2004) *J Am Chem Soc* 126(18):5851–5858
24. Sakai N, Fukuda K, Shibata T, Ebina Y, Takada K, Sasaki T (2006) *J Phys Chem B* 110(12):6198–6203
25. Shibata T, Sakai N, Fukuda K, Ebina Y, Sasaki T (2007) *Phys Chem Chem Phys* 9(19):2413–2420
26. Aruna ST, Tirosch S, Zaban A (2000) *J Mater Chem* 10(10):2388–2391
27. Kaper H, Endres F, Djerdj I, Antonietti M, Smarsly BM, Maier J, Hu Y-S (2007) *Small* 3(10):1753–1763
28. Li YL, Ishigaki T (2002) *Thin Solid Films* 407(1–2):79–85
29. Wang CC, Ying JY (1999) *Chem Mater* 11(11):3113–3120
30. Shen XJ, Zhang JL, Tian BZ (2011) *J Hazard Mater* 192(2):651–657
31. Cassaignon S, Koelsch M, Jolivet J-P (2007) *J Phys Chem Solids* 68(5–6):695–700
32. Cassaignon S, Koelsch M, Jolivet J-P (2007) *J Mater Sci* 42(16):6689–6695
33. Kao L-H, Hsu T-C, Lu H-Y (2007) *J Colloid Interface Sci* 316(1):160–167
34. Pottier AS, Cassaignon S, Chaneac C, Villain F, Tronc E, Jolivet J-P (2003) *J Mater Chem* 13(4):877–882
35. Sugimoto T (2004) *Chem Commun* 2004(14):1584–1585
36. Sugimoto T, Zhou X, Muramatsu A (2003) *J Colloid Interface Sci* 259(1):53–61
37. Niederberger M, Garnweitner G, Krumeich F, Nesper R, Colfen H, Antonietti M (2004) *Chem Mater* 16(7):1202–1208
38. Trentler TJ, Denler TE, Bertone JF, Agrawal A, Colvin VL (1999) *J Am Chem Soc* 121(7):1613–1614
39. Yang GX, Zhuang HR, Biswas P (1996) *Nanostruct Mater* 7(6):675–689
40. Buonsanti R, Grillo V, Carlino E, Giannini C, Kipp T, Cingolani R, Cozzoli PD (2008) *J Am Chem Soc* 130(33):11223–11233
41. Deng Q, Wei M, Hong Z, Ding X, Jiang L, Wei K (2010) *Curr Nanosci* 6(5):479–482
42. Keesmann I, Anorg Z (1966) *Allg Chem* 346(1–2):30–43
43. Kobayashi M, Tomita K, Petrykin V, Yoshimura M, Kakihana M (2008) *J Mater Sci* 43(7):2158–2162
44. Kominami H, Ishii Y, Kohno M, Konishi S, Kera Y, Ohtani B (2003) *Catal Lett* 91 (1–2):41–47
45. Kominami H, Kohno M, Kera Y (2000) *J Mater Chem* 10(5):1151–1156
46. Bhavne RC, Lee BI (2007) *Mater Sci Eng A* 467(1–2):146–149
47. Inada M, Iwamoto K, Enomoto N, Hojo J (2011) *J Ceram Soc Jpn* 119(1390):451–455
48. Pottier A, Chaneac C, Tronc E, Mazerolles L, Jolivet JP (2001) *J Mater Chem* 11(4):1116–1121
49. Durupthy O, Bill J, Aldinger F (2007) *Cryst Growth Des* 7(12):2696–2704
50. Yang HG, Sun CH, Qiao SZ, Zou J, Liu G, Smith SC, Cheng HM, Lu GQ (2008) *Nature* 453(7195):638–642
51. Kandiel TA, Feldhoff A, Robben L, Dillert R, Bahnemann DW (2010) *Chem Mater* 22(6):2050–2060
52. Wu B, Guo C, Zheng N, Xie Z, Stucky GD (2008) *J Am Chem Soc* 130(51):17563–17567
53. Roy P, Berger S, Schmuki P (2011) *Angew Chem Int Ed* 50(13):2904–2939
54. Chemseddine A, Moritz T (1999) *Eur J Inorg Chem* 2:235–245
55. Moritz T, Reiss J, Diesner K, Su D, Chemseddine A (1997) *J Phys Chem B* 101(41): 8052–8053
56. Kanie K, Sugimoto T (2004) *Chem Commun* 14:1584–1585
57. Miao L, Tanemura S, Toh S, Kaneko K, Tanemura M (2004) *J Cryst Growth* 264(1–3): 246–252
58. Lin Y, Wu GS, Yuan XY, Xie T, Zhang LD (2003) *J Phys Condens Matter* 15(17): 2917–2922

59. Crepaldi EL, Soler-Illia G, Grosso D, Cagnol F, Ribot F, Sanchez C (2003) *J Am Chem Soc* 125(32):9770–9786
60. Sakatani Y, Grosso D, Nicole L, Boissiere C, Soler-Illia G, Sanchez C (2006) *J Mater Chem* 16(1):77–82
61. Andersson M, Osterlund L, Ljungstrom S, Palmqvist A (2002) *J Phys Chem B* 106(41):10674–10679
62. Yener HB, Sarkaya S, Helvacı SS (2010) *Trends Colloid Interface Sci* Xxiii 137:23–28
63. Kim CS, Moon BK, Park JH, Choi BC, Seo HJ (2003) *J Cryst Growth* 257(3–4):309–315
64. Yao BD, Chan YF, Zhang XY, Zhang WF, Yang ZY, Wang N (2003) *Appl Phys Lett* 82(2):281–283
65. Zhang YX, Li GH, Jin YX, Zhang Y, Zhang J, Zhang LD (2002) *Chem Phys Lett* 365(3–4):300–304
66. Desmoulins-Krawiec S, Aymonier C, Loppinet-Serani A, Weill F, Gorse S, Etourneau J, Cansell F (2004) *J Mater Chem* 14(2):228–232
67. Dong X, Tao J, Li Y, Zhu H (2010) *Appl Surf Sci* 256(8):2532–2538
68. Macak JM, Zlamal M, Krysa J, Schmuki P (2007) *Small* 3(2):300–304
69. Jiang L-C, Zhang W-D (2009) *Electroanalysis* 21(8):988–993
70. El-Sheikh AH, Newman AP, Al-Daffae H, Phull S, Cresswell N, York S (2004) *Surf Coat Technol* 187(2–3):284–292
71. Pradhan SK, Reucroft PJ, Yang FQ, Dozier A (2003) *J Cryst Growth* 256(1–2):83–88
72. Seifried S, Winterer M, Hahn H (2000) *Chem Vap Depos* 6(5):239–244
73. Anuradha TV, Ranganathan S (2007) *Bull Mater Sci* 30(3):263–269
74. Ding Z, Lu GQ, Greenfield PF (2000) *J Phys Chem B* 104(19):4815–4820
75. Fujishima A, Hashimoto K, Watanabe T (1999) *TiO<sub>2</sub> photocatalysis: fundamentals and applications*. BKC Inc., Tokyo
76. Schindler KM, Kunst M (1990) *J Phys Chem* 94(21):8222–8226
77. Tanaka K, Capule MFV, Hisanaga T (1991) *Chem Phys Lett* 187(1–2):73–76
78. Gratzel M, Rotzinger FP (1985) *Chem Phys Lett* 118(5):474–477
79. Tang H, Prasad K, Sanjines R, Schmid PE, Levy F (1994) *J Appl Phys* 75(4):2042–2047
80. Di Paola A, Addamo M, Bellardita M, Cazzanelli E, Palmisano L (2007) *Thin Solid Films* 515(7–8):3527–3529
81. Di Paola A, Cufalo G, Addamo M, Ellardita MB, Campostrini R, Ischia M, Ceccato R, Palmisano L (2008) *Colloids Surf A* 317(1–3):366–376
82. Ohtani B, Handa J, Nishimoto S, Kagiya T (1985) *Chem Phys Lett* 120(3):292–294
83. Iskandar F, Nandiyanto ABD, Yun KM, Hogan CJ Jr, Okuyama K, Biswas P (2007) *Adv Mater* 19(10):1408–1412
84. Li FB, Li XZ, Hou MF (2004) *Appl Catal B* 48(3):185–194
85. Hurum DC, Agrios AG, Gray KA, Rajh T, Thurnauer MC (2003) *J Phys Chem B* 107(19):4545–4549
86. Evgenidou E, Bizani E, Christophoridis C, Fytianos K (2007) *Chemosphere* 68(10):1877–1882
87. Gutfraind R, Sheintuch M, Avnir D (1991) *J Chem Phys* 95(8):6100–6111
88. Tsai SC, Chung YW (1984) *J Catal* 86(1):231–234
89. Zhang ZB, Wang CC, Zakaria R, Ying JY (1998) *J Phys Chem B* 102(52):10871–10878
90. Tomkiewicz M (2000) *Catal Today* 58(2–3):115–123
91. Maeda M, Watanabe T (2007) *Surf Coat Technol* 201(22–23):9309–9312
92. Tian S, Yang H, Cui M, Shi R, Zhao H, Wang X, Wang X, Zhang L (2011) *Appl Phys A* 104(1):149–158
93. Luis AM, Neves MC, Mendonca MH, Monteiro OC (2011) *Mater Chem Phys* 125(1–2):20–25
94. Agrios AG, Pichat P, *Photochem J* (2006) *Photobiology A* 180(1–2):130–135
95. Watts RJ, Kong S, Orr MP, Miller GC, Henry BE (1995) *Water Res* 29(1):95–100
96. Zhu XL, Yuan CW, Bao YC, Yang JH, Wu YZ (2005) *J Mol Catal A Chem* 229(1–2):95–105



97. Mogyorosi K, Balazs N, Sranko DF, Tombacz E, Dekany I, Oszko A, Sipos P, Dombi A (2010) *Appl Catal B* 96(3–4):577–585
98. Yang XH, Li Z, Sun C, Yang HG, Li C (2011) *Chem Mater* 23(15):3486–3494
99. Gong XQ, Selloni A (2005) *J Phys Chem B* 109(42):19560–19562
100. Liu S, Yu J, Jaroniec M (2010) *J Am Chem Soc* 132(34):11914–11916
101. Liu S, Yu J, Jaroniec M (2011) *Chem Mater* 23(18):4085–4093
102. Tachikawa T, Yamashita S, Majima T (2011) *J Am Chem Soc* 133(18):7197–7204
103. Zhao X, Jin W, Cai J, Ye J, Li Z, Ma Y, Xie J, Qi L (2011) *Adv Funct Mater* 21(18):3554–3563
104. Choi WY, Termin A, Hoffmann MR (1994) *J Phys Chem* 98(51):13669–13679
105. Asahi R, Morikawa T, Ohwaki T, Aoki K, Taga Y (2001) *Science* 293(5528):269–271
106. Hagfeldt A, Gratzel M (1995) *Chem Rev* 95(1):49–68
107. Oregan B, Gratzel M (1991) *Nature* 353(6346):737–740
108. Rajeshwar K, de Tacconi NR, Chenthamarakshan CR (2001) *Chem Mater* 13(9):2765–2782
109. Takeuchi M, Yamashita H, Matsuoka M, Anpo M, Hirao T, Itoh N, Iwamoto N (2000) *Catal Lett* 67(2–4):135–137
110. Wang YQ, Cheng HM, Hao YZ, Ma JM, Li WH, Cai SM (1999) *Thin Solid Films* 349(1–2):120–125
111. Bessekhouad Y, Robert D, Weber JV, Chaoui N, Photochem J (2004) *Photobiology A* 167(1):49–57
112. Burda C, Lou YB, Chen XB, Samia ACS, Stout J, Gole JL (2003) *Nano Lett* 3(8):1049–1051
113. Nakamura R, Tanaka T, Nakato Y (2004) *J Phys Chem B* 108(30):10617–10620
114. Diwald O, Thompson TL, Goralski EG, Walck SD, Yates JT (2004) *J Phys Chem B* 108(1):52–57
115. Jin TS, Ma YR, Sun X, Liang D, Li TS (2000) *J Chem Res Synop* 2:96–97
116. Corma A, Martinez A, Martinez C (1996) *Appl Catal A* 144(1–2):249–268
117. Zaban A, Micic OI, Gregg BA, Nozik AJ (1998) *Langmuir* 14(12):3153–3156
118. Vogel R, Hoyer P, Weller H (1994) *J Phys Chem* 98(12):3183–3188
119. Vinodgopal K, Kamat PV (1995) *Environ Sci Technol* 29(3):841–845
120. Ranjit KT, Viswanathan B (1997) *J Photochem Photobiol A* 108(1):79–84
121. Ohtani B, Zhang SW, Ogita T, Nishimoto S, Kagiya T (1993) *J Photochem Photobiol A* 71(2):195–198
122. Vorontsov AV, Savinov EN, Jin ZS (1999) *J Photochem Photobiol A* 125(1–3):113–117
123. Calza P, Pelizzetti E, Minero C (2005) *J Appl Electrochem* 35(7–8):665–673
124. Emeline AV, Ryabchuk VK, Serpone N (2005) *J Phys Chem B* 109(39):18515–18521
125. Fujishima A, Zhang X, Tryk DA (2008) *Surf Sci Rep* 63(12):515–582
126. Tachikawa T, Fujitsuka M, Majima T (2007) *J Phys Chem C* 111(14):5259–5275
127. Thompson TL, Yates JT Jr (2006) *Chem Rev* 106(10):4428–4453
128. Yates JT (2009) *Surf Sci* 603(10–12):1605–1612
129. Henderson MA (2011) *Surf Sci Rep* 66(6–7):185–297
130. Murakami M, Matsumoto Y, Nakajima K, Makino T, Segawa Y, Chikyw T, Ahmet P, Kawasaki M, Koinuma H (2001) *Appl Phys Lett* 78(18):2664–2666
131. Leytner S, Hupp JT (2000) *Chem Phys Lett* 330(3, 4):231–236
132. Wang Z, Helmersson U, Kall P-O (2002) *Thin Solid Films* 405(1–2):50–54
133. Tang H, Berger H, Schmid PE, Levy F (1994) *Solid State Commun* 92(3):267–271
134. Asahi R, Taga Y, Mannstadt W, Freeman AJ (2000) *Phys Rev B Condens Matter Mater Phys* 61(11):7459–7465
135. Qu Z-W, Kroes G-J (2006) *J Phys Chem B* 110(18):8998–9007
136. Satoh N, Nakashima T, Kamikura K, Yamamoto K (2008) *Nat Nanotechnol* 3(2):106–111
137. Szarko JM, Neubauer A, Bartelt A, Socaciu-Siebert L, Birkner F, Schwarzburg K, Hannappel T, Eichberger R (2008) *J Phys Chem C* 112(28):10542–10552
138. Zou B, Xiao L, Li T, Zhao J, Lai Z, Gu S (1991) *Appl Phys Lett* 59(15):1826–1828

139. Du Y, Deskins NA, Zhang Z, Dohnalek Z, Dupuis M, Lyubinetsky I (2009) *J Phys Chem C* 113(2):666–671
140. Lee HS, Woo CS, Youn BK, Kim SY, Oh ST, Sung YE, Lee HI (2005) *Top Catal* 35 (3–4):255–260 Park JH, Park OO, Kim S (2006) *Appl Phys Lett* 89(16):163106–163108
142. Khomenko VM, Langer K, Rager H, Fett A (1998) *Phys Chem Miner* 25(5):338–346
143. Komaguchi K, Maruoka T, Nakano H, Imae I, Ooyama Y, Harima Y (2010) *J Phys Chem C* 114(2):1240–1245
144. Umebayashi T, Yamaki T, Itoh H, Asai K (2002) *J Phys Chem Solids* 63(10):1909–1920
145. Choi J, Park H, Hoffmann MR (2010) *J Phys Chem C* 114(2):783–792
146. Maeda M, Watanabe T (2006) *J Electrochem Soc* 153(3):C186–C189
147. Balcerski W, Ryu SY, Hoffmann MR (2007) *J Phys Chem C* 111(42):15357–15362
148. Turner GM, Beard MC, Schmittenmaer CA (2002) *J Phys Chem B* 106(45):11716–11719
149. Shen Q, Katayama K, Sawada T, Yamaguchi M, Kumagai Y, Toyoda T (2006) *Chem Phys Lett* 419(4–6):464–468
150. Abuabara SG, Rego LGC, Batista VS (2005) *J Am Chem Soc* 127(51):18234–18242
151. Rego LGC, Batista VS (2003) *J Am Chem Soc* 125(26):7989–7997 Hendry E, Wang F, Shan J, Heinz TF, Bonn M (2004) *Phys Rev B* 69(8):081101(R)–081104(R)
153. Deskins NA, Dupuis M (2009) *J Phys Chem C* 113(1):346–358
154. Henderson MA, White JM, Uetsuka H, Onishi H (2003) *J Am Chem Soc* 125(49):14974–14975
155. Deskins NA, Rousseau R, Dupuis M (2009) *J Phys Chem C* 113(33):14583–14586
156. Ikeda S, Sugiyama N, Murakami S-Y, Kominami H, Kera Y, Noguchi H, Uosaki K, Torimoto T, Ohtani B (2003) *Phys Chem Chem Phys* 5(4):778–783
157. Kuznetsov AI, Kameneva O, Alexandrov A, Bityurin N, Marteau P, Chhor K, Sanchez C, Kanaev A (2005) *Phys Rev E Stat Nonlin Soft Matter Phys* 71(2 Pt 1):021403
158. Hurum DC, Gray KA, Rajh T, Thurnauer MC (2005) *J Phys Chem B* 109(2):977–980
159. Martin ST, Herrmann H, Choi W, Hoffmann MR (1994) *J Chem Soc Faraday Trans* 90(21):3315–3322
160. Colbeau-Justin C, Kunst M, Huguenin D (2003) *J Mater Sci* 38(11):2429–2437
161. Tang H, Prasad K, Sanilines R, Schmid PE, Levy F (1994) *J Appl Phys* 75(4):2042–2047
162. Yamakata A, Ishibashi T-A, Onishi H (2007) *Chem Phys* 339(1–3):133–137
163. Katoh R, Huijser A, Hara K, Savenije TJ, Siebbeles LDA (2007) *J Phys Chem C* 111(28):10741–10746
164. Serpone N, Lawless D, Khairutdinov R, Pelizzetti E (1995) *J Phys Chem* 99(45):16655–16661
165. Asahi T, Furube A, Masuhara H (1997) *Chem Phys Lett* 275(3, 4):234–238
166. Rabani J, Yamashita K, Ushida K, Stark J, Kira A (1998) *J Phys Chem B* 102(10):1689–1695
167. Furube A, Asahi T, Masuhara H, Yamashita H, Anpo M (2001) *Res Chem Intermed* 27(1–2):177–187
168. Ryabchuk V (2004) *Int J Photoenergy* 6(3):95–113
169. Wendt S, Sprunger PT, Lira E, Madsen GKH, Li Z, Hansen JO, Matthiesen J, Blekinge-Rasmussen A, Laegsgaard E, Hammer B, Besenbacher F (2008) *Science* 320(5884):1755–1759
170. Babay PA, Emilio CA, Ferreyra RE, Gautier EA, Gettar RT, Litter MI (2001) *Water Sci Technol* 44(5):179–185
171. Lisachenko AA, Mikhailov RV, Basov LL, Shelimov BN, Che M (2007) *J Phys Chem C* 111(39):14440–14447
172. Wu W-C, Chuang C-C, Lin J-L (2000) *J Phys Chem B* 104(36):8719–8724
173. Arana J, Dona-Rodriguez JM, Cabo CGI, Gonzalez-Diaz O, Herrera-Melian JA, Perez-Pena J (2004) *Appl Catal B* 53(4):221–232
174. Micic OI, Zhang Y, Cromack KR, Trifunac AD, Thurnauer MC (1993) *J Phys Chem* 97(50):13284–13288
175. Liao L-F, Wu W-C, Chen C-Y, Lin J-L (2001) *J Phys Chem B* 105(32):7678–7685

176. Jayaweera PM, Quah EL, Idriss H (2007) *J Phys Chem C* 111(4):1764–1769
177. Sobczynski A, Duczmal L, Zmudzinski W (2004) *J Mol Catal A Chem* 213(2):225–230
178. Jenkins CA, Murphy DM (1999) *J Phys Chem B* 103(6):1019–1026
179. Carter E, Carley AF, Murphy DM (2007) *ChemPhysChem* 8(1):113–123
180. Coronado JM, Kataoka S, Tejedor-Tejedor I, Anderson MA (2003) *J Catal* 219(1):219–230
181. Kraeutler B, Bard AJ (1978) *J Am Chem Soc* 100(7):2239–2240
182. Henderson MA (2005) *J Phys Chem B* 109(24):12062–12070
183. Blount MC, Kim DH, Falconer JL (2001) *Environ Sci Technol* 35(14):2988–2994
184. Wilson JN, Idriss H (2002) *J Am Chem Soc* 124(38):11284–11285
185. Ajmera AA, Sawant SB, Pangarkar VG, Beenackers AACM (2002) *Chem Eng Technol* 25(2):173–180
186. Boarini P, Carassiti V, Maldotti A, Amadelli R (1998) *Langmuir* 14(8):2080–2085
187. Gondal MA, Hameed A, Yamani ZH, Arfaj A (2004) *Chem Phys Lett* 392(4–6):372–377
188. Shi D, Feng Y, Zhong S (2004) *Catal Today* 98(4):505–509
189. Ohno T, Tokieda K, Higashida S, Matsumura M (2003) *Appl Catal A* 244(2):383–391
190. Coronado JM, Soria J (2007) *Catal Today* 123(1–4):37–41
191. Stark J, Rabani J (1999) *J Phys Chem B* 103(40):8524–8531
192. Yamazoe S, Okumura T, Hitomi Y, Shishido T, Tanaka T (2007) *J Phys Chem C* 111(29):11077–11085
193. Emeline AV, Serpone N (2002) *J Phys Chem B* 106(47):12221–12226
194. Lukaski AC, Muggli DS (2003) *Catal Lett* 89(1–2):129–138
195. Mills A, Wang J (1999) *J Photochem Photobiol A* 127(1–3):123–134
196. Serpone N, Sauve G, Koch R, Tahiri H, Pichat P, Piccinini P, Pelizzetti E, Hidaka H (1996) *J Photochem Photobiol A* 94(2–3):191–203
197. Pichat P, Vannier S, Dussaud J, Rubis J-P (2004) *Sol Energy* 77(5):533–542
198. Chatzisyameon E, Stypas E, Bousios S, Xekoukoulotakis NP, Mantzavinos D (2008) *J Hazard Mater* 154(1–3):1090–1097
199. Rodrigues AC, Boroski M, Shimada NS, Garcia JC, Nozaki J, Hioka N (2008) *J Photochem Photobiol A* 194(1):1–10
200. Alinsafi A, Evenou F, Abdulkarim EM, Pons MN, Zahraa O, Benhammou A, Yaacoubi A, Nejmeddine A (2007) *Dyes Pigm* 74(2):439–445
201. Antoniadis A, Takavakoglou V, Zalidis G, Poullos I (2007) *Catal Today* 124(3–4):260–265
202. Lachheb H, Puzenat E, Houas A, Ksibi M, Elaloui E, Guillard C, Herrmann J-M (2002) *Appl Catal B* 39(1):75–90
203. Sauer T, Cesconeto Neto G, José HJ, Moreira RFP (2002) *J Photochem Photobiol A* 149(1–3):147–154
204. Mounir B, Pons MN, Zahraa O, Yaacoubi A, Benhammou A (2007) *J Hazard Mater* 148(3):513–520
205. Gonçalves MST, Pinto EMS, Nkeonye P, Oliveira-Campos AMF (2005) *Dyes Pigm* 64(2):135–139
206. Herrmann J-M, Guillard C (2000) *Comptes Rendus de l'Académie des Sciences—Series IIC—Chemistry* 3(6):417–422
207. Devipriya S, Yesodharan S (2005) *Sol Energy Mater Sol Cells* 86(3):309–348
208. Guillard C, Bui T-H, Felix C, Moules V, Lina B, Lejeune P (2008) *C R Chim* 11(1–2):107–113
209. Pigeot-Rémy S, Simonet F, Errazuriz-Cerda E, Lazzaroni JC, Atlan D, Guillard C (2011) *Appl Catal B* 104(3–4):390–398
210. Rizzo L (2009) *J Hazard Mater* 165(1–3):48–51
211. Rizzo L, Meric S, Kassinos D, Guida M, Russo F, Belgiorno V (2009) *Water Res* 43(4):979–988
212. Giraldo AL, Peñuela GA, Torres-Palma RA, Pino NJ, Palominos RA, Mansilla HD (2010) *Water Res* 44(18):5158–5167
213. Elmolla ES, Chaudhuri M (2010) *Desalination* 252(1–3):46–52

214. Guillard C, Beaugiraud B, Dutriez C, Herrmann J-M, Jaffrezic H, Jaffrezic-Renault N, Lacroix M (2002) *Appl Catal B* 39(4):331–342
215. Guillard C, Disdier J, Monnet C, Dussaud J, Malato S, Blanco J, Maldonado MI, Herrmann J-M (2003) *Appl Catal B* 46(2):319–332
216. Alfano OM, Bahnemann D, Cassano AE, Dillert R, Goslich R (2000) *Catal Today* 58(2–3):199–230
217. Bahnemann D (2004) *Sol Energy* 77(5):445–459
218. Malato S, Blanco J, Vidal A, Richter C (2002) *Appl Catal B Environ* 37(1):1–15
219. Blake DM (2001) Bibliography of work on photocatalytic removal of hazardous compounds from water and air, NREL/TP-510-31319, National Renewable Energy Laboratory, Golden, Colorado
220. Zhang L, Anderson WA, Zhang ZJ (2006) *Chem Eng J (Lausanne)* 121(2–3):125–134
221. Miller LW, Anderson MA (1998) *J Adv Oxid Technol* 3(3):238–242
222. Danion A, Disdier J, Guillard C, Abdelmalek F, Jaffrezic-Renault N (2004) *Appl Catal B* 52(3):213–223
223. Molinari R, Mungari M, Drioli E, Di Paola A, Loddo V, Palmisano L, Schiavello M (2000) *Catal Today* 55(1–2):71–78
224. Sclafani A, Sciascia A, Rizzuti L (1999) *J Adv Oxid Technol* 4(1):91–96
225. Fabiyi ME, Skelton RL (1999) *J Photochem Photobiol A* 129(1–2):17–24
226. Danion A, Disdier J, Guillard C, Jaffrezic-Renault N (2007) *J Photochem Photobiol A* 190(1):135–140
227. Cassano AE, Alfano OM (2000) *Catal Today* 58(2–3):167–197
228. Brandi RJ, Rintoul G, Alfano OM, Cassano AE (2002) *Catal Today* 76(2–4):161–175
229. Brandi RJ, Citroni MA, Alfano OM, Cassano AE (2003) *Chem Eng Sci* 58(3–6):979–985
230. Moreira J, Serrano B, Ortiz A, de Lasa H (2010) *Ind Eng Chem Res* 49(21):10524–10534